Evaluation of Novel and Low-Cost Materials for Bipolar Plates in PEM Fuel Cells

Kevin Campbell Desrosiers

Thesis submitted to the faculty of the Virginia Polytechnic Institute and State University in partial fulfillment of the requirements for the degree of

Master of Science
in
Mechanical Engineering

Committee Members:

Dr. Douglas J. Nelson – Advisor, ME
Dr. Michael W. Ellis – ME
Dr. Michael R. von Spakovsky – ME

September 16, 2002
Blacksburg, Virginia

Keywords: Fuel Cell, PEMFC, Separator Plates, Injection Molding, Test Stand, Graphite, Composite

Evaluation of Novel and Low-Cost Materials for Bipolar Plates in PEM Fuel Cells

Kevin Campbell Desrosiers

(ABSTRACT)

Bipolar plate material and fabrication costs make up a significant fraction of the total cost in a polymer electrolyte membrane fuel cell stack. In an attempt to reduce these costs, a novel manufacturing method was developed for use with composite materials. Conductive fillers were mixed with a polypropylene binder and molded into single cell monopolar plates. A fuel cell test stand, capable of testing six cells simultaneously, was used for long-term corrosion testing. In-situ tests took place in 5 cm^2 active area fuel cells with cathode humidification. Using data from test cells containing graphite monopolar plates as a baseline, two composite formulations, were able to produce power at 66-79% of the baseline power. Power output from one cell remained in this range for over 200 hours, while the other sample experienced surface oxidation and eventually failed. With improvements in part conductivity coming from conductive polymers, this manufacturing technique holds the promise of producing monopolar and bipolar plates that could eventually be scaled up for use in fuel cell stacks.

Acknowledgments

I would like to thank Holly Grammar, Eric Kruszewski, Dr. Douglas J. Nelson, and Directed Technologies Inc. for their invaluable support during this research.

The Virginia Center for Innovative Technologies and the National Science Foundation provided funding for this project.

Dedication

To Mom, who encouraged me to follow my dreams and pursue an advanced degree, but who couldn't be there when I returned. I miss you.

Table of Contents

List of Figures

List of Tables

1 Introduction

Proton Exchange Membrane Fuel Cells, also known as Polymer Electrolyte Membrane Fuel Cells (PEMFCs), use hydrogen to generate electrical power. Vehicles, buildings, and portable electronic devices can all potentially derive their power from fuel cells. Currently the cost of fuel cells is prohibitive for most applications, but research seeks to lower these costs through advances in design and materials usage. Because bipolar plates make up a large portion of a fuel cell's cost and weight, improvements in bipolar plate technology could help fuel cells become a viable alternative to the internal combustion engine. This section covers a brief history and operation of fuel cells, the importance of bipolar plates in fuel cells, and the scope of this bipolar plate research.

1.1 History and Operation of Fuel Cells

William Grove first demonstrated the concept of a fuel cell in 1839. By passing a current through a dilute acid solution using platinum electrodes, he was able to electrolyze water into hydrogen and oxygen. After some time, Grove replaced the current source with an ammeter. He found that a weak current was flowing back through the cell. The hydrogen and oxygen were recombining. Although the concept of a fuel cell had been known for over 100 years, it was not until the 1960s that fuel cells started to be used regularly in the American space program. Recently, the need for more efficient automobiles and cleaner burning fuels has led to more intense research into alternative energy systems. Today's PEM fuel cells are more complicated than Grove's first experiment, but the process still works in the same way.

Fuel cells are energy conversion devices and will run for extended periods, as long as fuel is in continuous supply. As shown in Figure 1-1, hydrogen is supplied to the anode where the gas encounters the membrane-electrode-assembly (MEA). The MEA, impregnated with platinum, initiates the electrochemical reaction allowing protons to pass through the selectively permeable membrane, while forcing electrons to move along an outside circuit. It is in this outside circuit that current can be used to power any number of electrical devices. Continuing through the cell, the oxygen combines with the

protons and electrons at the cathode, and forms water. In most cases, the membrane must be sufficiently hydrated in order to conduct protons. This hydration can be maintained by humidifying the cathode air stream (as in this research), or both reactant gas steams.

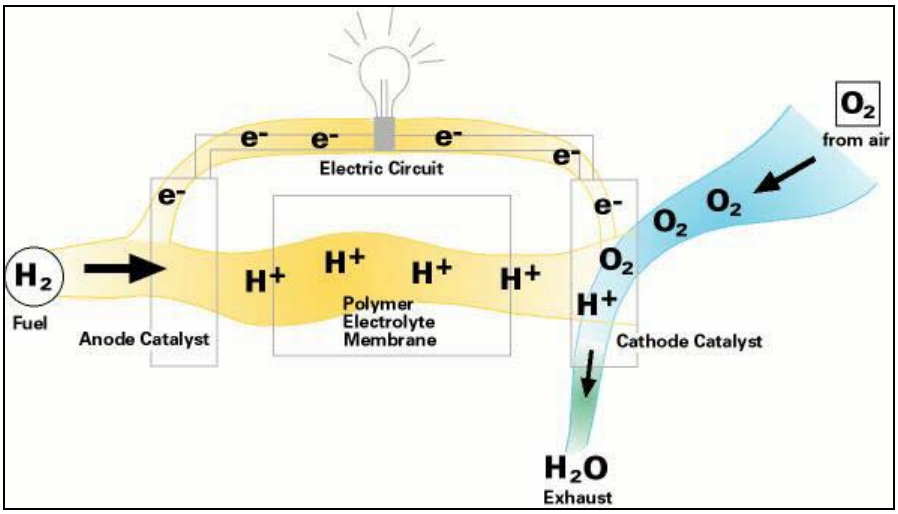

Figure 1-1: Flow of products and reactants in a fuel cell (Fuel Cells 2000/U.S. Department of Energy).

The electrochemical reactions that occur inside the fuel cell (as represented by Figure 1-1) are shown in equations 1.1 (anode) and 1.2 (cathode) with the net synthesis reaction shown in equation 1.3:

$$2H_2 \rightarrow 4H^+ + 4\,e^- \quad (1.1)$$

$$O_2 + 4\,e^- + 4H^+ \rightarrow 2H_2O \quad (1.2)$$

$$2H_2 + O_2 \rightarrow 2H_2O \quad (1.3)$$

Since a single cell can only produce close to 1 volt, many cells can be assembled together in series to form a fuel cell stack. By combining stacks in series and parallel, different voltages and power outputs can be obtained. A single fuel cell stack, containing many cells, appears in Figure 1-2. A few individual cells could be used to power low wattage devices such as cell phones, while a vehicle requiring 60 kW of power might require hundreds of cells. The individual cells in a stack are composed of an MEA sandwiched

between two bipolar plates. These bipolar plates play an important role in a fuel cell stack, which will be discussed in the next section.

Figure 1-2: A 10 kW fuel cell stack (Honeywell).

1.2 Importance of Bipolar Plates

Bipolar plates serve many functions in a fuel cell stack. They are responsible for distributing reactant gasses, removing product water, supporting the membranes, conducting electrons, and housing coolant channels. Distributing hydrogen and oxygen evenly over the MEA and removing product water is the job of the plate flow field (see Figure 1-3). This design is often an intricate serpentine pattern of channels only a few millimeters in width and depth. The plates themselves conduct electrons from the anode of one cell to the cathode of the next and serve as rigid support structures for the membranes. Narrow flow fields permit maximum surface area of the bipolar plate to contact the membrane, which allows for better electron conduction and more even gas distribution over the membrane. In large stacks, coolant channels are often incorporated in the bipolar plate design.

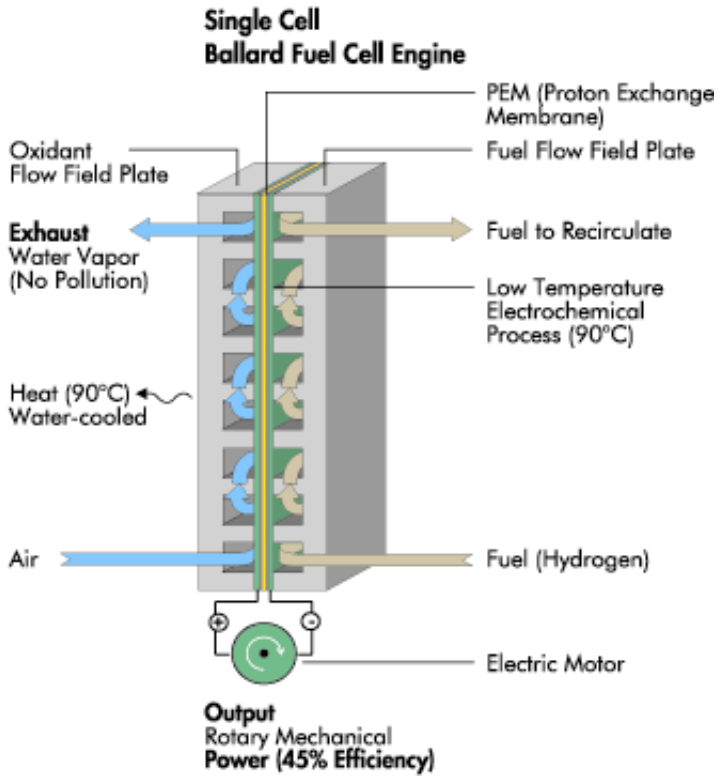

Figure 1-3: Flow paths in fuel cell bipolar plates (Ballard Power Systems).

Most fuel cells in operation today contain bipolar plates made out of some form of graphite. Some material properties of graphite make it well suited for use in fuel cells, although other properties make the material less than ideal. Graphite is conductive, resistant to corrosion, resistant to high temperatures, and impermeable to reactant gases (if thick enough).

Bipolar plates are currently manufactured by machining intricate flows channels into sheets of graphite. Since fuel cell stacks can be made up of hundreds of plates, the machining cost alone can add a significant amount to the overall cost of a stack. Being quite brittle, graphite plates are also easily chipped during machining often ruining them before use. Because graphite is not very dense, bipolar plates must be at least a few millimeters thick to keep the reactant gases separated. This extra thickness not only adds resistance to the flow of electrons, but also adds to the weight and size of the fuel cell stack.

1.3 Scope of Research

The scope of this research is to design a bipolar plate that is cost effective, is lighter, and performs as well as current graphite bipolar plates. More specifically, we hope that these new bipolar plates could eventually replace graphite as the material of choice. In order to be considered for use, the new plates must meet several criteria:

1) high conductivity
2) high mechanical strength, and
3) high corrosion resistance.

Other criteria that are already met by the materials and manufacturing process used in this research include having low density (relative to metal), being impermeable to reactant gases, and being easy to manufacture. When these criteria are met, the new bipolar plates will be able to compete with graphite bipolar plates that are currently used in fuel cells.

In a fuel cell stack containing many individual cells in series, the separator plates are bipolar, meaning the negative side of one plate is the positive side of the next plate. Since the test cells in this research were made up of only one cell, the plates are in fact monopolar.

To improve conductivity, a reduction in plate material resistance (which causes voltage drop) is essential. There are three main types of polarizations, or voltage losses, in a PEM fuel cell. They include: (1) activation losses – which are due to slow reactions at the electrodes (governed by the Tafel equation); (2) ohmic losses – caused by resistance to electron or ion flow (governed by Ohm's Law); and (3) concentration losses – which occur when reactants are consumed at the reaction sites as fast as possible and further increases in reactant bulk concentration lead to diminishing returns. The first two types of losses are evident in Figure 1-4. The red (dashed line) non-linear section represents the region of predominant activation losses, and the blue (hollow diamonds) linear section represents the region of predominant ohmic losses. The slope of the linear region is a direct measurement of the ohmic losses in the fuel cell. Reducing the resistance of the bipolar plates will minimize voltage loss and be reflected on polarization curves as a decrease in slope. Therefore, higher amounts of current can flow in a cell creating less of a voltage drop.

In this research, all new sample plates were corrosion tested at stack operating conditions in a 5 cm^2 (active area) single cell, fuel cell. In previous work[1], six Poco graphite cells were run for around 1000 hours each in order to establish a data baseline. The data obtained from these endurance tests allowed performance comparisons between the Poco graphite and composite cells.

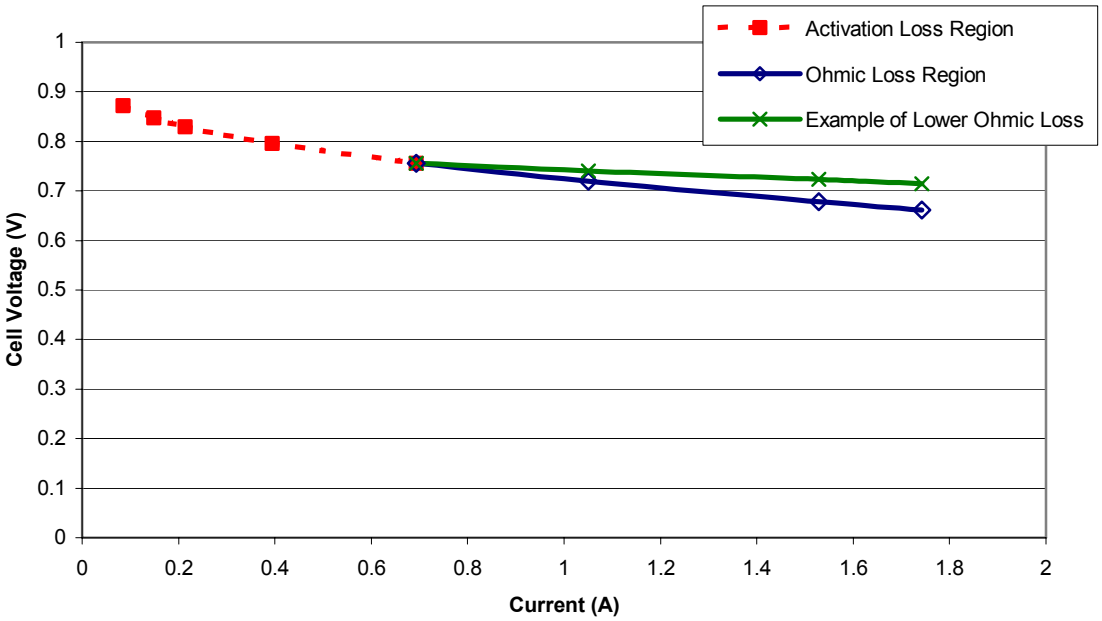

Figure 1-4: Polarization curve for Poco graphite showing activation and ohmic loss regions.

Several types of materials have been tested in bipolar plate research experiments. Stainless steel, titanium, and carbon composites have all performed relatively well compared with machined graphite, but tend to be heavy and involve lengthy processing procedures. In our research, we are trying to enhance the conductivity of polymer composites, improve their mechanical strength, and improve resistance to corrosion. Goals outlined in the Small Business Innovative Research (SBIR) report associated with this research include: (1) total electrical conductivity normal to the face of the bipolar plate of 2 S/cm for automotive applications and 10 S/cm for stationary applications; and (2) corrosion resistance compatible with a total cell peak power loss of less than 20% in 5,000 hours for automotive use and 6% a year for stationary power applications. These composite materials will allow the plates to be molded in a commercial plastics process, reducing cost, production run time, and post processing.

2. Literature Review

Considerable effort on the part of researchers, in government and private labs, has gone into the development and testing of new bipolar plate materials and manufacturing processes. This literature review covers progress made in the development of bipolar plates classified according to composites, metallics, and combinations.

2.1 Graphite Composites

Besman et al.[2] tested a carbon composite material molded from phenolic resin and carbon fibers. This low-cost slurry method produced a highly porous material with hermetically sealed edges. Having a porous volume allows the material to act as a diffuser and flow field in one, which avoids separate layers of material. A slurry was first vacuum molded at 50°C and then carbonized under nitrogen and graphitized at 1050°C and 2800°C, respectively. One face and the sides of the 2 mm thick sample plate were then hermetically sealed in a graphite furnace under CH_4 at 1400°C. The resultant material was both thin and light weight with high electrical conductivity. At this point in their research, Besman et al. had not machined or molded flow fields and inlet/outlet holes into the material.

A novel, composite graphite material, developed by SGL Technik GmbH, was tested by Scholta et al.[3] The 1.5 mm bipolar plate was tested in a fuel cell under a pure H_2/O_2 environment without humidification. Polarization results after 120 hours of testing, at 80°C, showed minimal decrease in cell performance, and the bipolar plates remained impermeable to gas leakage. Testing for plate endurance capabilities had not yet taken place, and methods to lower the material resistance were being sought.

Vinyl ester resins, filled with varying amounts of graphite powders, were investigated by Busick and Wilson.[4] Thermoset resins, which are permanently bonded after molding (can not be re-melted), can be removed from molds while hot. This removal allows for faster processing, as opposed to thermoplastic materials, which must be cooled somewhat before removing them from the mold. Benefits from using vinyl

esters include low production and materials costs, and high corrosion resistance. The bipolar plates made from these materials were both strong and lightweight, and no detectable H_2 permeated the material. Busick and Wilson's research found that compression molding produced bipolar plates that performed almost as well as machined graphite or steel plates, although longer processing times might lead to higher costs.

2.2 Metallics

Metal bipolar plates can perform as well as machined graphite, but the tendency for insulating oxide layers to build up on metal surfaces (reducing electrical conductivity) and the possibility of corrosion in the fuel cell environment have limited their use. In 1997, Hornung and Kappelt [5] examined the use of corrosion resistant iron-based alloys to possibly replace the gold-plated, nickel-based alloys that were currently in use. Their research found that iron based alloys were comparable to nickel based alloys in terms of polarization, but that the iron-based alloys were subject to some corrosion in 0.1 mol/l HCl solution. According to Hornung and Kappelt, only the gold-plated nickel samples had low enough contact resistance[a] to be used successfully in a fuel cell.

Work by Davies et al.[6] sought to compare the performance characteristics between bipolar plates made of Poco graphite (considered an industry standard), titanium, and 310 and 316 stainless steel. Each material (except graphite) has the tendency to form an oxidation layer, which can increase internal resistance in a fuel cell. Davies et al. found that cell potential decreased in the following order: Poco > 310 SS > Ti > 316 SS. This decrease was based on an increase in surface layer thickness. A significant finding from their work was that 310 stainless steel performed much better than 316 stainless steel (316 had been used more widely in fuel cell tests). Long-term tests also revealed that cells running with titanium bipolar plates actually decreased in performance. This decrease in performance was due to an increase of the oxide layer under operating conditions.

[a] Interfaces between materials in a fuel cell such as the bipolar plate, gas diffusion layer, and membrane all create contact resistance. Cell compaction force can overcome some of this interfacial contact resistance, but altering material properties such as by applying low resistance surface coatings can help eliminate even more contact resistance.

Titanium, 316L stainless steel (lower carbon content than 316), and gold-plated aluminum were tested as bipolar plate materials by Hentall et al.,[7] and performance data was compared with the Poco graphite and GRAFOIL® standards. GRAFOIL® (now known as GRAFCELL®) is a flexible graphite sheet developed by Graftech Inc. This material has excellent conductivity and corrosion resistance. The titanium plates were made up of many individual plates with different flow patterns, which were diffusion bonded. Diffusion bonding leaves a clean and distortion free joint. This method also allows water-cooling channels to be designed into the plates. Titanium plates performed as well as Poco plates, and since titanium is stronger, a thinner plate can be used. Cells with 316L SS did not perform as well as graphite; but when the 316L SS was gold plated, these bipolar plates out performed graphite quite significantly. The gold plated 316L SS plates also proved to be less expensive than titanium; however, a higher material density reduces the gravimetric power density (W/kg) of stacks using these plates. A coating of titanium nitride was applied to the stainless steel and titanium samples. This coating decreased voltage loss and improved the performance of the steel plates to that of graphite. When gold plated aluminum was used, it initially performed almost as well as graphite, although performance decreased soon after the layer of gold separated from the plate. Further analysis revealed contamination of the membrane by aluminum. These materials were also compared with the performance of GRAFOIL®. The GRAFOIL® had superior performance over all materials tested. Since it lacks mechanical strength, external support is required.

Several alloys of stainless steel were tested by Makkus et al.[8] Bipolar plates were constructed from the following materials listed by their Material UNS code: 1.4439, 1.4404 (316 L), 1.4541, 1.4529, and 1.3974. Two proprietary alloys, A and B, were also tested and compared with a cell using graphite plates. Tests were performed using high cell compaction pressure along with direct MEA/bipolar plate contact, and low cell compaction pressure with no direct contact between the MEA and bipolar plate. They found that direct contact between the MEA and the bipolar plate resulted in higher contaminant levels in the MEA. In all cases, more contaminants came from bipolar plates located at the anode side of the test cell. Because alloys 1.4439 and 1.4541 had visible pitting in them, they were not investigated further.

Makkus[8] also found that compaction pressure had a large influence on cell contact resistance. His team used a gold wire located between the E-tek carbon cloth backing and the membrane to measure the voltage drop from the wire to the bipolar plate (in tests of 30 bars, and 4 bars). This measurement also included resistance imparted from the backing layer, but gave a reasonable measurement of the contact resistance between the bipolar plate and MEA. A significant finding of their research is that the period of open circuit voltage (OCV) greatly influences cell degradation. In separate experiments, fuel cell performance would slightly improve after short OCV periods of two to five minutes, while a performance drop of 2.5% would occur after 30 minutes at OCV. Short periods of OCV allow the membrane to become more evenly hydrated (after periods of operation), whereas reactant gasses start to dry out the membrane after longer periods of OCV.

Davies et al.[9] further investigated the use of stainless steel (SS) alloys as potential bipolar plate materials. Cells tested for over 3000 hours showed no significant corrosion and proved that SS could operate in the fuel cell environment without degradation (thus, eliminating the need for expensive coatings). The three alloys of stainless steel tested, from best performance to worst performance, were 904L > 310 > 316. This order was due to the increasing oxide layer on each alloy, respectively. Titanium, which is much less dense than stainless steel, still allows for thin plates and therefore a lighter stack. However, the titanium bipolar plates rapidly built up an oxidation layer, which caused the test cell to fail. Sample plates made of stainless steel had no decrease in performance over time. Davies et al. also found significant contact resistance existed between the bipolar plate and gas diffusion layer (GDL) interface. In their publication, they noted that the bulk resistivity of stainless steel is much less than that of the oxide layer. This note would indicate that some sort of resistance reducing coating might benefit bipolar plates made of metal.

Further work by Hodgson et al.[10] examined short and long term performance of cells assembled with surface treated titanium, bipolar plates. Their research found that a special surface coating prevented the insulating oxide layer from building up and decreased the contact resistance of the plate. Test results showed better performance over untreated 316 stainless steel. However, the thickness of their proprietary FC5 coating was

found to be important, since a decrease in the conductivity of the bipolar plate with the application of too much additional material would result.

Corrosion tests were performed in heated sulfuric and hydrofluoric acid while passing a current through the plates. Measuring the contact resistance before and after corrosion testing provided durability information on the FC5 coating. These tests did not affect contact resistance or show any signs of corroding the metal. Additional measurements of compaction force and contact resistance showed the FC5 treated plates to perform as well as machined graphite, far exceeding the performance of uncoated 316 stainless steel. A significant finding of the work by Hodgson et al. was that cells containing the coated titanium plates produced a higher voltage than cells containing the stainless steel plates. In addition, no metal ions from the bipolar plates were found in the MEA after use.

Low cost coatings for SS 316L were investigated by Wind et al.[11] Testing uncoated SS and graphite plates gave them baseline performance data to compare with data from tests of proprietary coatings. Flow fields were etched into the SS plates, and coatings were applied using various deposition techniques. Both the air and hydrogen were humidified to a dew point of 70°C in these experiments. In-situ measurement of resistances between the bipolar plates and electrodes was accomplished with voltage probes inside the cell. Ex-situ analysis of an uncoated cathode-side plate revealed an oxide layer had built up, which increased the resistivity of the cell causing poor performance. Analysis of the MEA revealed a high concentration of nickel. Further tests of gold plated SS 316L showed that MEA contamination was significantly reduced and cell performance did not decrease due to oxide layer build up. Sample plates with coatings less expensive than gold were also tested in-situ. Results showed four of the six samples achieved almost zero voltage loss over the length of the 500 hour tests. Select coatings were then tested for 1000 hours with minimal performance decay suggesting that SS 316L bipolar plates with protective coatings are good candidates for use in PEM fuel cells. A summary of this literature review can be seen in Table 2-1.

Table 2-1: Summary of significant findings in bipolar plate research.

Principal Investigator	Year	Materials	Significant Findings
Besmann[2]	1998	Phenolic resin/carbon composite	Thin, lightweight material, with high conductivity
Scholta[3]	1999	Graphite composite	Minimal decrease in cell performance after 120 hours
Busick[4]	1999	Vinyl ester resins w/ graphite powders	Compression molded parts performed almost as well as machined graphite
Hornung[5]	1997	Iron based alloys	Only Au plated iron alloys had low enough contact resistance for bipolar plates
Davies[6]	1999	Ti, 310 SS, 316 SS, Poco graphite	310 SS better than 316 SS, and untreated Ti plates build oxide layer, cause cell to fail
Hentall[7]	1999	Ti, 316L SS, Al (both Au plated), Poco graphite	Au plated 316L performed better than Poco graphite
Makkus[8]	1999	Various SS alloys	Direct contact of MEA and bipolar plate leads to more MEA contamination
Davies[9]	2000	Ti, SS alloys (904L, 310, 316)	904L SS performed better than 310 and 316
Hodgson[10]	2001	Ti (w/ active surface coating) and 316 SS	Coating on Ti reduced contact resistance, and outperformed untreated 316 SS
Wind[11]	2002	SS 316L w/ Au and low cost proprietary coatings, graphite	Four of six low cost coatings prevented oxide buildup with performance similar to graphite

3 Testing Procedure

This section describes the assembly of the fuel cell body and the preparation of the fuel cell test stand designed by Directed Technologies, Inc. Previously in this research, graphite monopolar plates were tested in these fuel cells.[1] During this phase of the research, composite monopolar plates were tested.

3.1 Assembly of Fuel Cell

In this assembly, a half cell is composed of three distinct pieces: an aluminum end plate; a glass-filled, Teflon electrode holder; and a gold-plated, copper current collector. Each piece fits together to form the outer portion of the fuel cell. This assembly allows reactants and products to flow to and from the membrane at the cell's center.

The end plates are machined from 6061 T6 aluminum. They serve as surfaces for adhesive silicone heaters to heat each side of the fuel cell to a constant temperature of 70°C. The Teflon electrode holders were designed to be non-conductive and to withstand temperatures of up to 120°C. Because an area of about 1-inch diameter has been machined out of the Teflon, the "lollipop" shaped current collectors can fit snuggly within the cell. A tight fit is necessary for minimal contact resistance between the monopolar plate and the current collector.

The next layer in the cell is the monopolar plate. A sample plate fits on top of the previously mentioned current collector. Molded into the plate is a flow field that allows the reactant gasses to flow over the membrane and allows water to flow away from the reaction areas. Drilling small holes, 1/32 inch, at each end of the flow field, allows the water and gasses to enter and exit the membrane area. These holes align with holes in the current collectors and the electrode holder. A small fitting on the outside of the cell connects the cell to the gas supply while fittings on the other side of the cell exhaust product water and gasses to the atmosphere. Shown in Figure 3-1 is a half cell with a Poco graphite monopolar plate.

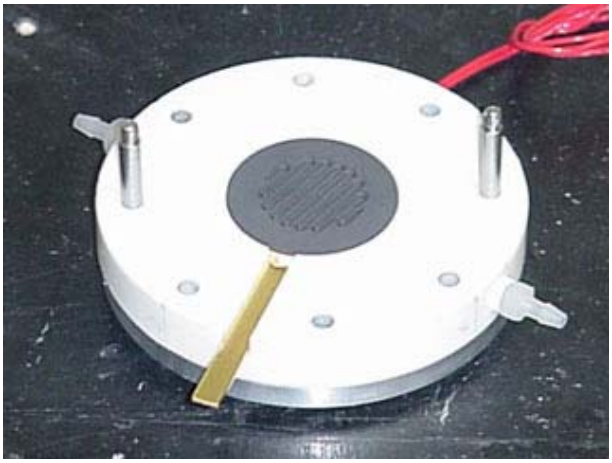

Figure 3-1: Half of a test fuel cell with monopolar plate and current collector.

The membrane and other conductive layers are located inside the fuel cell body, where the electrochemical reaction takes place. This group of materials (Figure 3-2) is made up of a gas diffusion layer (GDL), a mesoporous layer, and the membrane electrode assembly (MEA). The MEA (PRIMEA® 5510) and mesoporous layer are supplied by W. L. Gore. In order for reactant gasses to be evenly dispersed over the MEA, a layer of Spectracarb's 2050A GDL is placed on each side. This porous, graphitic, fiber mesh serves three functions: (1) allows gasses to diffuse evenly over the membrane, (2) allows product water to diffuse away from the membrane, and (3) conducts electrons away to be used for power. Because the graphite fibers in the GDL are quite small, they can damage the delicate membrane, which is 20 μm thick. The spongy mesoporous layer (also a GDL) not only protects the membrane from the carbon paper GDL, but also helps maintain hydration in the MEA. At high loads, significant water is produced in the membrane; however, at low loads, the membrane might start to dry out. The mesoporous layer allows the cell to operate in dryer conditions. Separating the hydrogen and air streams, while allowing protons to pass from the anode to cathode, is the job of the MEA. A small amount of platinum in the MEA decreases the activation energy required for the reaction to take place.

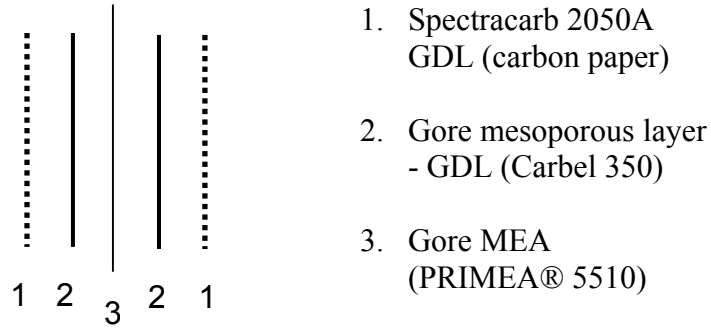

Figure 3-2: Diagram of inner fuel cell layers (adapted from Kruszewski)[1].

Before the fuel cell can be assembled, all parts must be cleaned and the membrane must be hydrated. The Teflon electrode holders and current collectors are each washed with double distilled, deionized water (DI water). The hydration process for the MEA must be followed very closely to ensure that membrane conditions will be the same in each fuel cell test. Because damage to the MEA and irritation of skin can occur if the membrane is not handled carefully, gloves and plastic tongs are used whenever a cell is prepared. A small beaker with DI water is heated to 60°C. After punching the membrane from the sheet of material (with a 1 3/4 inch die), it is placed in the water for 30 minutes. The water is then changed and reheated to 60°C, after which the membrane soaks for an additional 5 minutes. Not only is the DI water bath important for MEA hydration, but it also helps remove any acidic residue left in from the manufacture of the MEA. Acid species left on the MEA might promote corrosion of the composite monopolar plates in testing. While the membrane is in the water bath, the GDL and mesoporous layer can be punched from their respective sheets using the smaller 1 5/8 inch die. The mesoporous layer should be cut first, so that foreign material does not contaminate that sheet of material. In order to ease the alignment of the MEA with the other materials, a few tests were run using GDL and mesoporous material punched with the 1 5/8 inch die. These tests do not affect cell performance, but do leave some excess material around the edges of the cell.

After the MEA has been hydrated, the cell can be assembled. The monopolar plates are fitted inside the cell, on top of the current collectors. Alignment of the 1/32 inch flow holes is important, so that the cell is not starved of reactant gasses. Next, a

layer of GDL is placed over the monopolar plate, followed by a layer of mesoporous material. Then the MEA is placed on the stack. If alignment takes too long, then the MEA is placed back in the beaker of water for a few seconds to help maintain hydration. The remaining mesoporous layer and GDL are placed on the MEA. Two of the eight shoulder screws are left in the cell base, so that the other half of the cell can be placed over the sandwich of material with the proper alignment. Shown in Figure 3-3 is a completed cell.

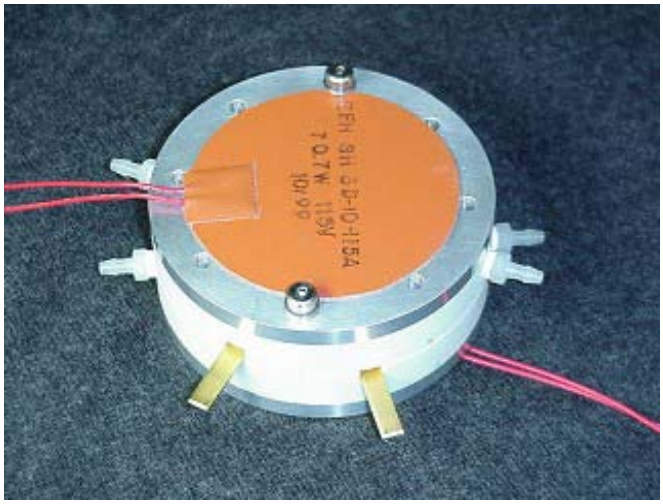

Figure 3-3: Assembled fuel cell body.

Cell compression is achieved by tightening the eight shoulder screws that squeeze against the aluminum end plates. Located at the base of each screw are two Bellville washers that aid in compression. Maintaining even pressure over the cell is important to prevent leaks that might decrease cell performance. In order to achieve even pressure, the screws are cross tightened by hand and then finished with a torque wrench to an appropriate level (4 – 6 inch-lbs).

3.2 Operation of Test Stand

The fuel cell test stand is composed of six individual stations (shown in Figure 3-4 a). Parameters that can be independently controlled at each station include airflow, hydrogen flow, cell temperature, and humidification temperature. A cathode

humidification column is shown in Figure 3-4 b. Humidification is achieved by passing the air stream (0.4 SLPM at 4.5 psig) through the water filled, one inch diameter stainless steel pipe, which is encircled by a one inch wide band heater at the base. Glass beads, measuring 0.5 cm in diameter, fill the first two inches of each column. These beads help increase turbulence in the water column and provide increased surface area for heat transfer to occur. The height of the water column varies from about eight inches down to three inches during the 12-14 hour interval in which it operates between refills.

(a) (b)

Figure 3-4: (a) An individual test station, and (b) cathode humidifier.

Measuring cell voltage and current at each station are two ammeters and one voltmeter. A digital ammeter provides an accurate measurement, while an analog meter serves as a visual check of the reading. Separate 5-volt power supplies power the digital meters for stations 1-3 and 4-6. The load that causes the fuel cell to change its power output is provided by a 10-100 ohm potentiometer. By changing the resistance on the cell, the current drawn increases and the voltage decreases. Data from this action forms a

polarization curve that can be compared with the curves from other cells to determine performance. A schematic of the electrical system is shown in Figure 3-5.

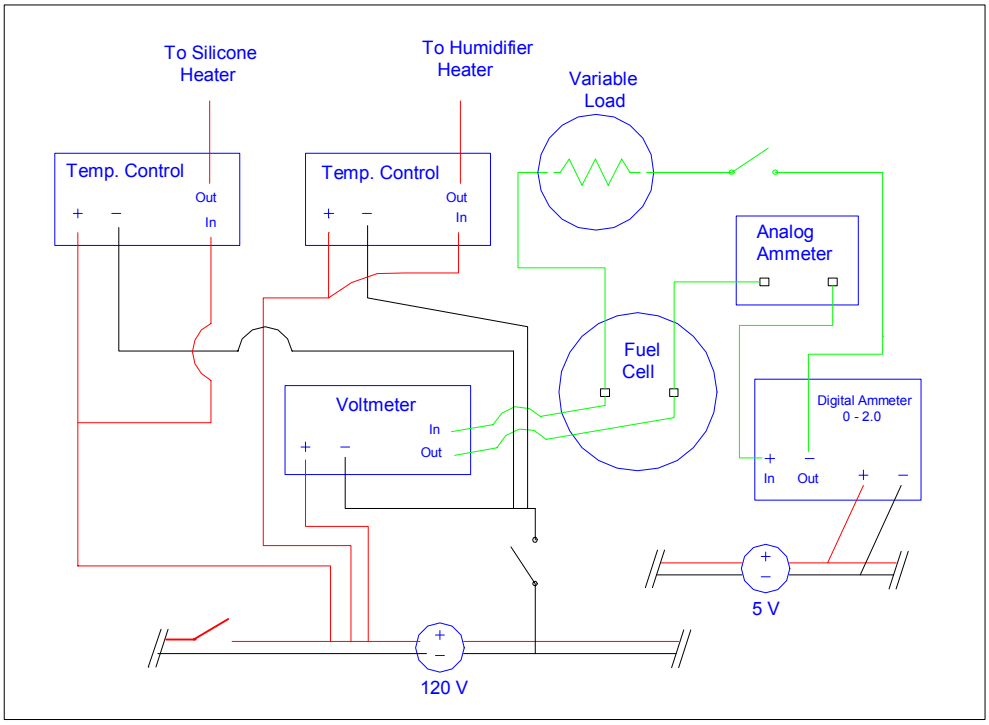

Figure 3-5: Electrical schematic for each station on the test stand (adapted from Kruszewski).[1]

Water balance in the fuel cells is important although only the cathode is humidified. Because the flow rate of hydrogen is low (0.054 SLPM at 15 psig), it will not dry the membrane as long as the cell is producing power. Water produced by the reaction and carried into the cell by the air stream is enough to keep the cell hydrated, due to the thin membrane promoting back diffusion to the anode. While the humidification chamber is heating up to 45°C, the cell is placed on the test stand and heated to 70°C. Simple PID temperature controllers are used to control heaters, and therefore, the temperature of all cells and humidification chambers. Assuming the air is close to saturation when leaving the humidifier, the relative humidity in the fuel cell is about 31%. The temperature of the humidified air is measured just as the air leaves the humidification chamber. Cell temperature is measured at a point central to the cell diameter, and just behind a gold plated current collector. To ensure that water does not condense inside the cell,

potentially damaging the membrane, the air is not connected to the humidifier until the cell has reached its operating temperature. After operating temperatures have been reached, the hydrogen flow is started slowly. A schematic showing gas system plumbing and the location of the humidifier is shown in Figure 3-6. Open circuit voltage (OCV), the highest possible voltage, is achieved within a few seconds. Then the load is applied, and the fuel cell begins to operate. The voltage drops from OCV to an operating voltage, which varies according to individual cell conditions.

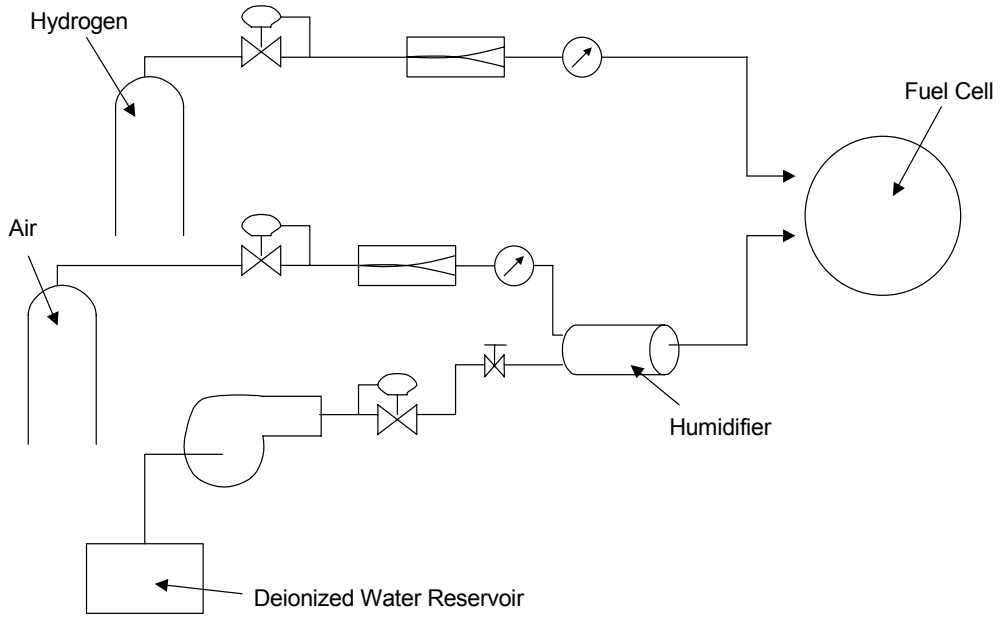

Figure 3-6: Gas system schematic.[1]

After the load has been applied to the fuel cell, a few sweeps of the potentiometer are made. Then the fuel cell is set at about one-quarter of full load and run over night as a break-in period. The following day, the load on the cell is set so that the cell will operate at about 0.7 volts for the duration of the endurance test. Day to day test stand maintenance is required in order to insure that test conditions remain relatively constant. Not only do the humidification chambers need to be refilled twice a day, but the gas flow rates also should be adjusted slightly to account for changes in tank pressure. Polarization data should be recorded when humidification water is at a level similar to that from the previous day's measurements. As the water column in the humidifier drops, the relative humidity likely drops, possibly explaining the fluctuation in power output (see chapter 4).

4 Test Results

This section describes the methods used to compare performance of the composite material monopolar plates to the baseline data obtained from the Poco graphite test cells. Also discussed are the test results and the inspection of monopolar plates for corrosion resistance.

4.1 Comparison of Composite and Baseline Data

In an earlier phase of this research, six PEM test cells (containing Poco graphite monopolar plates) were run in order to obtain baseline performance data.[1] This data was to be used for comparing the performance of the composite material monopolar plates. Since the performance of one cell degraded early in testing, only data from five of these cells (over 4300 hours) were used for comparison. Statistical analysis of this data set revealed that the standard deviation was high for some data points, so repeatability was a concern. The original 2-watt potentiometers became suspect for adding to much variability to the voltage and current signals (as shown by the hollow data points in Figure 4-1). Comparison of data obtained using a 4-watt potentiometer (as shown by the filled in data points) confirmed that the old data contained too much signal noise. The internal windings for the variable wiper were not very smooth and caused chatter when changing the load. All potentiometers were subsequently replaced with the new 4-watt style which had a tolerance of 5% and 280º of rotation.

Two additional Poco graphite test cells were then run for over 1000 hours each as a second set of baseline data. A performance degradation of the average Poco baseline curves can also be seen in Figure 4-1. Polarization curves and power curves for the Poco graphite cells can be seen in Appendix A. This loss of power output was an unexpected result and is most likely due to MEA degradation, or a build up of a film on the monopolar plates and current collectors. Since graphite is an inert and unreactive material inside a fuel cell, there was no reason to believe that these baseline monopolar plates would have corroded or degraded in any way. Analysis using an electron microscope showed evidence of materials on the surface of the plates that were not present at the start

of the tests. Post in-situ analysis of the MEAs was not performed. It is therefore likely that any residue build up was due to the humidification system.

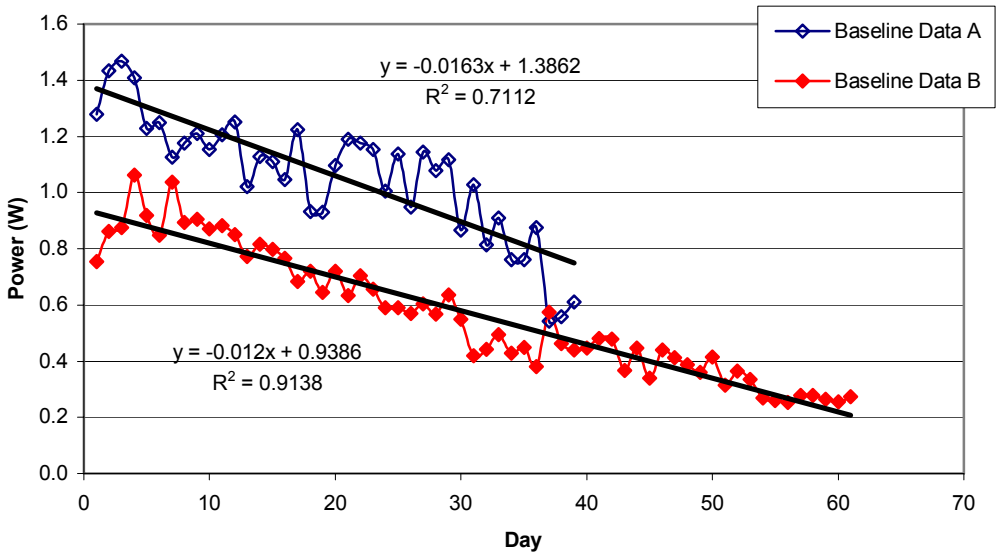

Figure 4-1: Power curve (at 0.6 volts) for Poco graphite baseline.

A possible source of cell performance degradation could have been the humidification chambers. The stainless steel pipe used to construct the chambers may not have been cleaned well when the test stand was initially constructed. Over time, the hot, wet, oxygen-rich environment could easily promote the formation of rust. Evidence of rust contamination was seen in the flow fields of only two monopolar plates. These were from two separate tests (same test station), so station #2 humidification chamber was rebuilt using a new section of pipe. The fact that a performance degradation was seen in almost all test cells from multiple test stations seems to indicate that contamination was a system wide problem, possibly from the humidification system.

The initial power output from the group A Poco cells is about 0.4 W higher than the group B cells. However, the rate of decay in power output is slightly higher for the first group (0.016 W/day) versus the second group (0.012 W/day). This seems to fit a general observation in testing namely, that cells with higher power output had higher performance decay rates.

Daily polarization data were taken for each test cell. Polarization curves show voltage versus current density. Curves for all composite samples can be seen in Appendix B. The current density, in A/cm^2, allows comparison between cells of different size. From the polarization curves, daily cell performance can be monitored, and the data used to compare potential power output from each test cell. Power curves were also created, using a linear regression of polarization data. A forecast function (linear regression) was used on the polarization data to calculate the power output at a given voltage. The cell power output was calculated at 0.7, 0.65, and 0.6 volts, which are voltages that a cell might encounter during typical automotive operation. Power curves provide a good visual indication of fuel cell performance.

Daily polarization curves (days 1-20 for simplicity) for one baseline cell can be seen in Figure 4-2. Each daily curve starts around the same value of 0.86 volts (at lowest load), but then as load is increased, the current density approaches 0.4 A/cm^2. However, the amount of current produced from the cell varies, as evidenced by the different slopes of the polarization curves. This variation is most likely due to fluctuations in membrane hydration and humidity chamber temperature. In addition, during the first few days of operation (membrane break-in period), cell power output increased slightly from its initial level of performance.

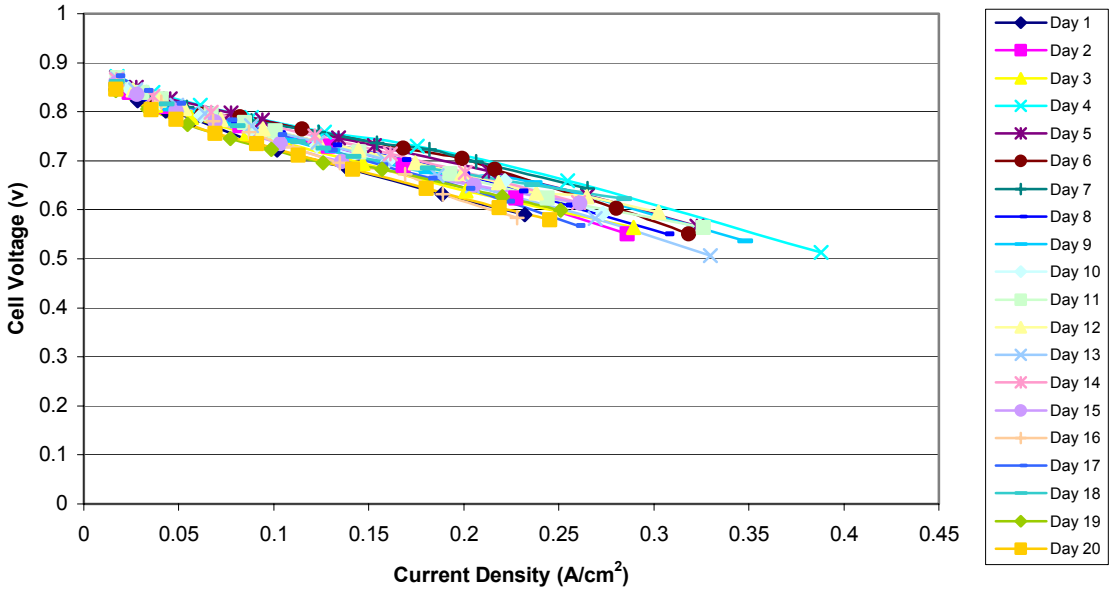

Figure 4-2: Polarization curves for a Poco baseline cell.

Eleven different composite samples were manufactured and tested during this research, although five of them were variations of the same material matrix.[12] Testing for all composite samples occurred under the same operating conditions and MEA configuration as the Poco graphite baseline cells.

There were three different processing methods used in this research. Each was a variation of a proprietary injection-coining operation. A standard process (SP) allowed the mold to be filled with the polymer mixture and then coined, while in the actual coining process (coin), a retracted mold was filled with the polymer mixture and then coined. Significant changes in conductivity were noted between identical composite mixtures processed with these two different methods. In the third process, a design of experiment (DOE) recommended changes in machine processing times for increased conductivity. Samples designated with the letter "a" are products of this change from the standard process, such as M15a. In all injection molding processes, a thin layer of polymer cools on contact with the mold. This skin core effect actually inhibits part conductivity since the conductive matrix would not be exposed to the outer layer of the molded part. Reducing this skin core layer was the objective of all variations in processing parameters. In order to remove as much skin core as possible without altering the sample matrix, some parts were subjected to surface abrasion (wet sanding). Surface abrasion increased sample conductivity by at least 0.8 S/cm in all cases. These samples are designated SM for "surface modified."

All composite samples contained a thermoplastic polypropylene binder (PP 7200) and different conductive fillers. These fillers included stainless steel fibers (SS 304), aluminum flakes (AL K109), aluminum fibers (Al 5056), carbon powder (4424), and carbon flakes (4955). Since polypropylene is nonconductive, a matrix of the conductive filler material was incorporated into the PP 7200 during the manufacturing process. By filling the polymer with various amounts of aluminum and carbon, or steel and carbon, properties such as fill fraction, material density, and conductivity could be altered. A Poco graphite plate is shown in Figure 4-3 along with samples C10 and M10.


(a) Poco graphite


(b) Sample C10


(c) Sample M10

Figure 4-3: Photos of (a) Poco graphite, (b) C10, and (c) M10 monopolar plates.

Most samples were not conductive, but eleven tested high enough to be placed on the test stand for further corrosion testing. Each individual sample contained an equal percentage (by volume) of carbon 4424 and carbon 4955, although these amounts differed from sample to sample. Table 4-1 shows the composite material combinations used in testing.

Table 4-1: Composite materials designations and compositions.

Sample	Composite Materials
C10	C/Polymer
M10	C/Al[a]/Polymer
M14	C/SS/Polymer
M15	C/SS/Polymer
M15a	C/SS/Polymer
M15a-SM	C/SS/Polymer
M15-coin	C/SS/Polymer
M15-coin/SM	C/SS/Polymer
M54	C/Al[b]/Polymer
M55-coin	C/Al[b]/Polymer
M55-coin/SM	C/Al[b]/Polymer
C = Carbon 4424/4955, SS = Stainless Steel 304, a = Aluminum 5056, b = Aluminum K109	

The only sample without metallic filler was formulation C10, which consisted of carbon and polymer. Many samples were manufactured using different fill fractions of carbon, but C10 (50% fill fraction) had the highest conductivity of the group at 1.2 Siemens/cm (S/cm). The in-situ fuel cell performance of C10 and the baseline performance of Poco graphite are shown in Figure 4-4. The average conductivity of sample C10 and Poco graphite was 1.2 and 15 S/cm, respectively. Overall, power output of C10 is significantly lower than Poco graphite. For example, the initial power output of C10 was 0.2 W whereas initial power output of Poco graphite was 0.7 W. The in-situ fuel cell performance of both samples reflects the measured conductivity results. An increase

in power observed for sample C10 (day 30) is due to replacement of the MEA in the test cell. Due to a shortage of MEAs at the time, C10 was tested with a previously used membrane. Since the membrane had already gone through a break-in period, no degradation was observed. However, replacing the MEA did not improve the cell performance to reasonable levels, so testing of C10 was discontinued. The absence of a downward slope in the C10 power curve could also be due to the low power output. Many samples with low power output had little noticeable degradation.

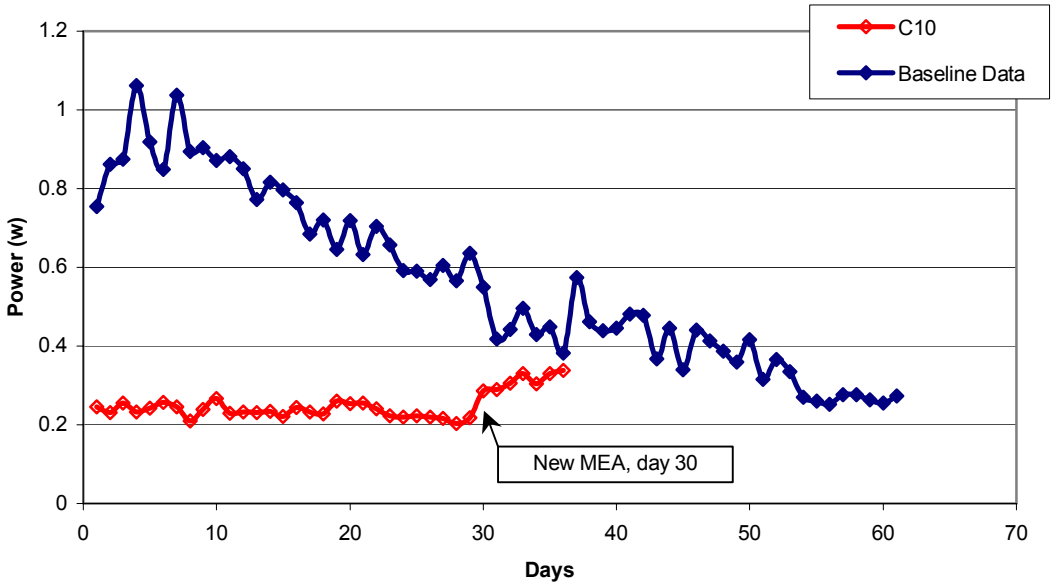

Figure 4-4: Power output for sample C10 (at 0.6 volts).

Sample M10 consisted of carbon, aluminum (Al 5056), and polymer. Average conductivity was measured at 2.0 S/cm. Although M10 had a higher conductivity than C10, the performance on the test stand did not reflect this fact. Initial power output was 0.22 W for C10 and 0.19 W for M10. After two days, the power output from sample M10 dropped to 0.15 W and continued a downward trend, so testing was halted. A comparison of the power output from a cell containing sample M10 to that of Poco graphite can be seen in Figure 4-5.

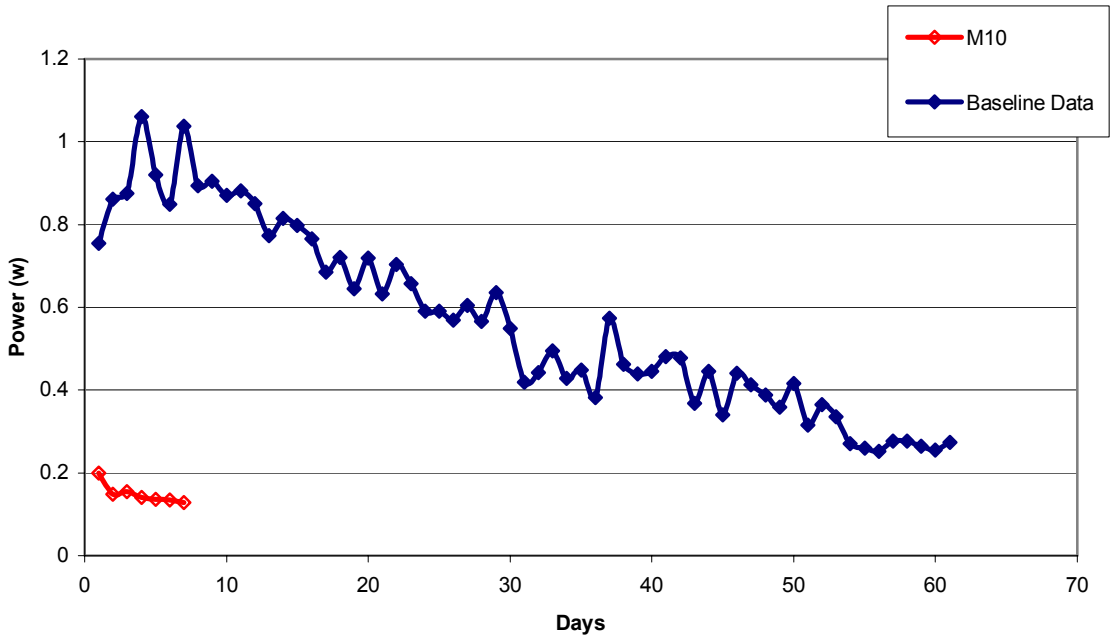

Figure 4-5: Power output for sample M10 (at 0.6 volts).

Three other aluminum-based samples were selected for further corrosion testing. Samples M54, M55 coin, and M55 coin/SM contained carbon, aluminum (Al K109), and polymer. Their average conductivities were 0.5, 2.6, and 3.0 S/cm, respectively. Producing only 0.14 watts of power, sample M54 failed to improve over 3 weeks of testing (as shown in Figure 4-6). Because samples M55-coin and M55-coin/SM had such high conductivities (in the sample lot), test stand power output was expected to be higher than that of other samples. However, sample M55-coin failed to produce any current or voltage once load was applied. In order to eliminate the possibility of a faulty MEA, that same MEA was removed from the M55-coin test cell and placed in a cell with Poco graphite monopolar plates. The MEA produced a steady current, confirming that the cell performance problem was likely due to the M55-coin monopolar plates. To be certain, another MEA was tested with sample M55-coin, resulting in zero current flow. Results were only slightly better with M55-coin/SM. This sample produced a small current (0.048 amps) at 0.489 volts, while at lowest load. Since the power output was so low, testing was not continued.

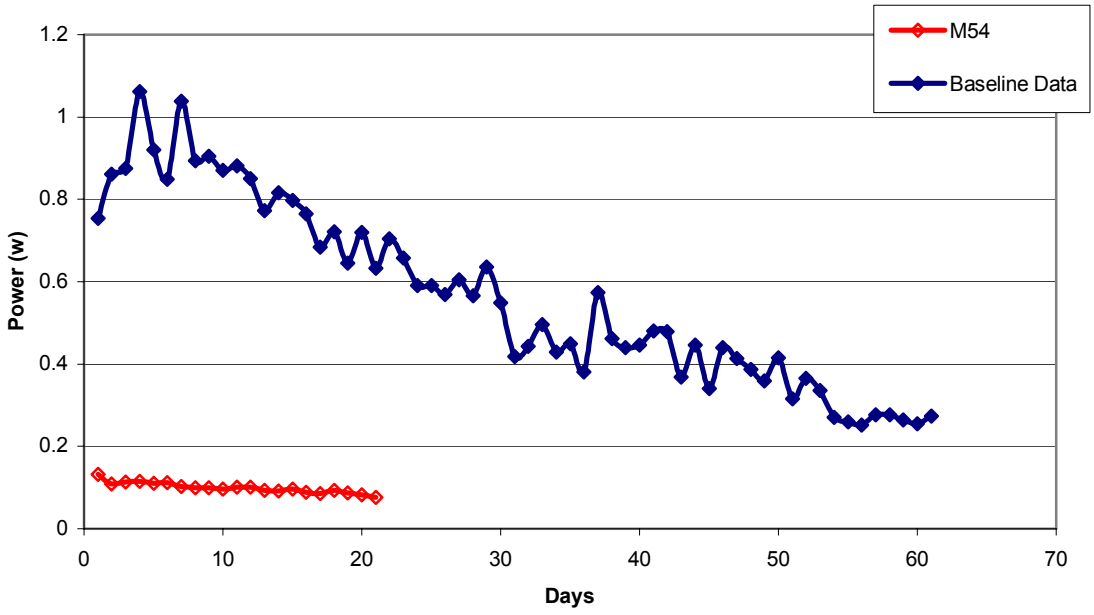

Figure 4-6: Power output for sample M54 (at 0.6 volts).

The final set of samples were all composed of carbon, steel (SS 304), and polymer. Sample M14 had a conductivity of 0.12 S/cm and initially had a power output of just 0.16 W. On day two of corrosion testing, the power output increased to 0.25 W, but gradually declined from there. Testing was suspended after 26 days. The M15 series of composite material proved to have the best power output from their test cells. Both M15 and M15a had the same average conductivity of 0.84 S/cm, but M15a had better performance after initially having a power output of 0.24 W versus 0.31 W for M15. The amount of power produced by sample M15a continued to increase over nine days of testing until the test stand had to be shut down for maintenance. This sample was producing 0.5 W at the time it was stopped. Composite sample M15 had a small increase in power output after the first day of testing, but started to oscillate between 0.4 and 0.21 W with a slight downward trend. This cell was stopped after 15 days.

A surface modified (SM) M15a sample, with a conductivity of 1.6 S/cm, had the highest power output of any sample tested in this research. Initial power output was about 0.62 W, with a few data points measuring as high as 0.7 W. Minimal performance degradation (0.005 W/day) was observed for sample M15a-SM. Finally, after 21 days of testing, a 17.5% performance decay was observed. Although this exceeded the maximum

level of acceptable performance degradation set in the SBIR Phase II report,[12] the improvement over other samples suggested that further advances could be made.

The final two composite samples, M15-coin and M15-coin/SM, had average conductivities of 2.4 and 2.8 S/cm, respectively. Although these samples had conductivities higher than that of composite M15a-SM, they did not perform as well on the test stand. Sample M15-coin had the second highest initial power output at 0.54 W. However, cell performance quickly degraded over 50% by day 10 of testing. Sample M15-coin/SM had the highest conductivity of all parts tested, but did not perform as well on the test stand as M15-coin or M15a-SM. The power output was very steady and did not decay by more than 0.01 W by the end of 15 days of testing. Graphical results from these samples are shown in Figure 4-7, while Table 4-2 provides a summary of the test results for the power output from each sample. Mean power output is for nine days of testing in the $5cm^2$ active area fuel cells.

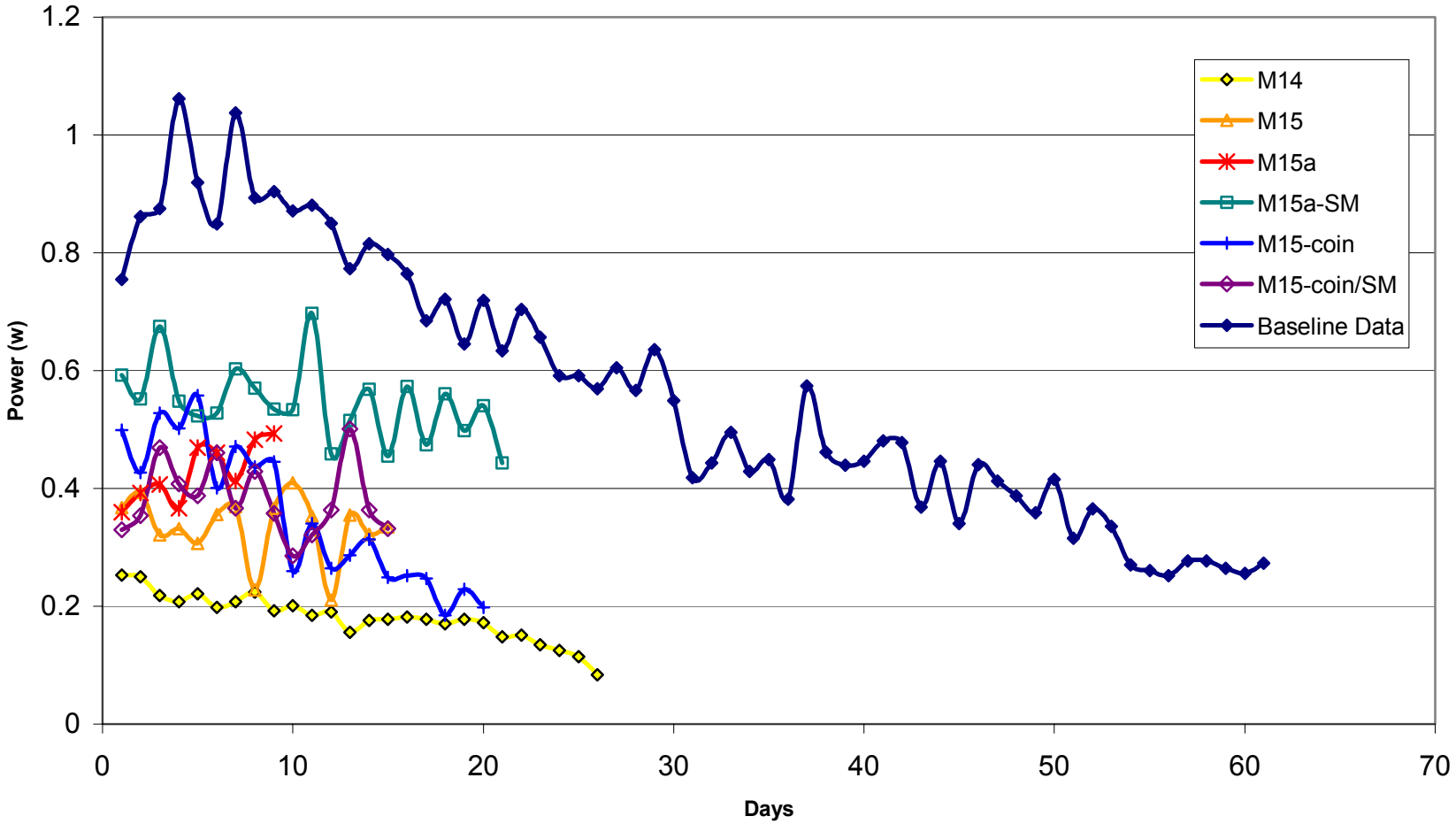

Figure 4-7: Power output for M14 and M15 series samples (at 0.6 volts).

Table 4-2: Composite sample conductivity and mean power output.

Sample	Composite Materials	Mean Conductivity (S/cm) before testing	Mean Power Output (W) at 0.6 volts (days 1-9)
C10	C/Polymer	1.2	0.24
M10	C/Al[a]/Polymer	2.0	0.15
M14	C/SS/Polymer	0.12	0.22
M15	C/SS/Polymer	0.25	0.34
M15a	C/SS/Polymer	0.84	0.43
M15a-SM	C/SS/Polymer	1.6	0.57
M15-coin	C/SS/Polymer	2.4	0.47
M15-coin/SM	C/SS/Polymer	2.8	0.40
M54	C/Al[b]/Polymer	0.5	0.11
M55-coin	C/Al[b]/Polymer	2.6	0
M55-coin/SM	C/Al[b]/Polymer	3.0	0
C = Carbon 4424/4955, SS = Stainless Steel 304, a = Aluminum 5056, b = Aluminum K109			

Despite the fact that most of the composite sample plates did not perform as well as the Poco graphite baseline, the power output was in most cases satisfactory. Test cells containing samples M15a-SM and M15-coin had initial power outputs of 66-79% of Poco graphite. These results were promising because the conductivities of these samples were only about 16% and 24%, respectively, of the conductivity of Poco graphite. Figure 4-8 shows the relative performance of all novel material plates as a percentage of the power output by the Poco graphite baseline test cells. Viewing the data in this format eliminates some of the performance degradation that all samples experienced from possible contamination by the test stand. As a result, the power output for most samples appears relatively steady for the duration of their testing. Only sample M15-coin experienced significant performance degradation when compared to the Poco graphite baseline. Table B.1 in Appendix B lists complete information on all composite samples tested in this research.

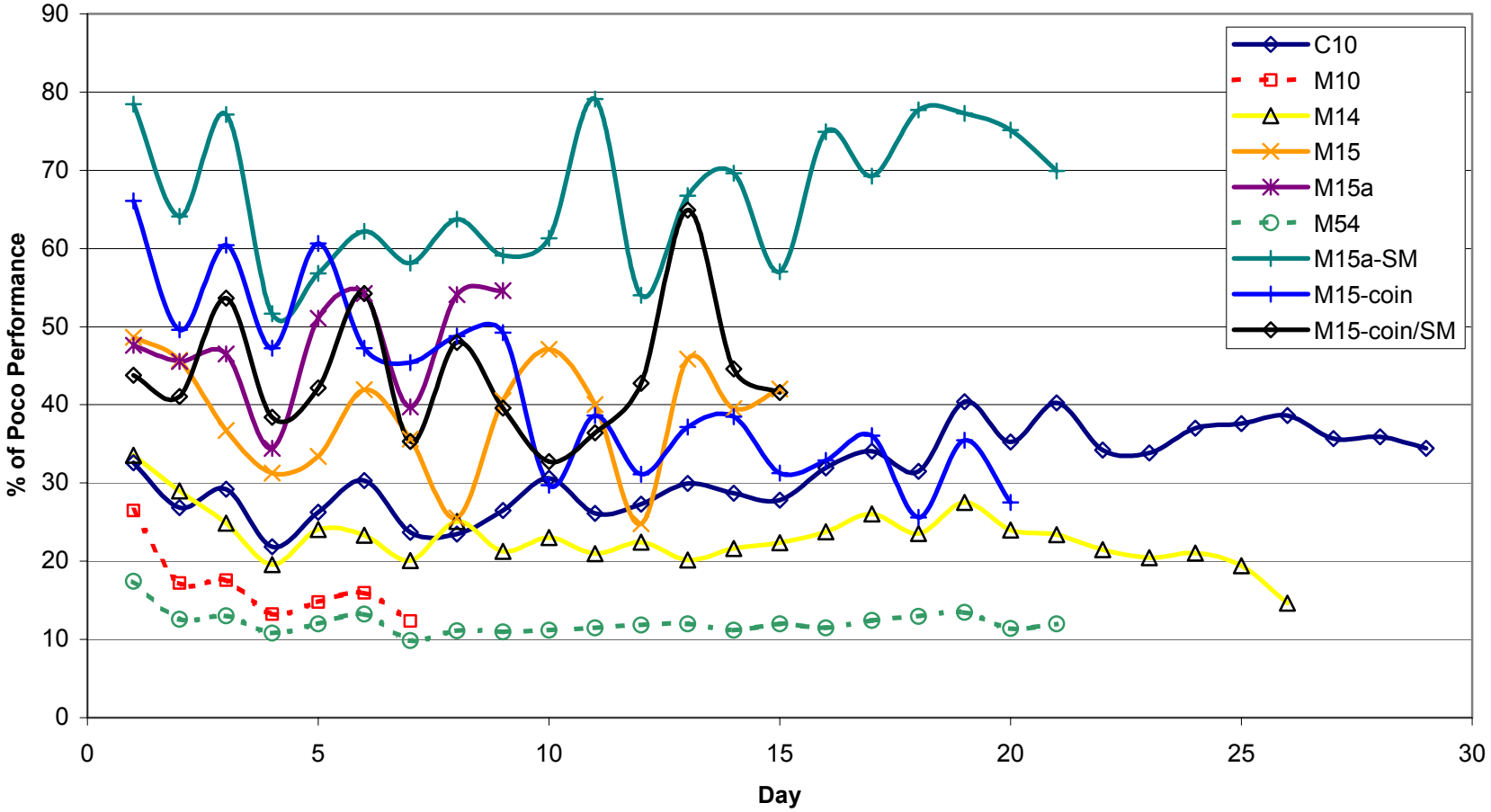

Figure 4-8: Test cell power output for novel material monopolar plates as a percentage of Poco graphite power output.

4.2 Inspection of Monopolar Plates for Corrosion Resistance

After each set of composite monopolar plates had completed in-situ fuel cell testing for a minimum of 150 hours, the test cell was taken apart and the plates were visually inspected. If corrosion was present, optical microscopy could be used to further analyze the sample plates. Many of the samples had small areas of a thin film on the backside of the plates (the side touching the gold plated current collectors) where water was collecting. It is uncertain whether this film had occurred because of a residue build up from the humidifiers, or if an oxide layer was forming due to operating conditions inside the fuel cell.

Sample C10 exhibited no corrosion since metallic fillers were not present in this sample. Minimal power output was observed for C10, but performance was steady and did not degrade over time. The reason that C10 performance did not decline can likely be explained by the fact that the MEA had been used previously in a Poco cell for an unknown number of days. Due to a shortage of membrane material at the time, the only option to test the new sample was the used MEA. Since the membrane had already gone through a break-in period, the decrease in performance seen in most other samples did not occur. After 29 days of testing, the C10 plates were cleaned and a new MEA was substituted (See Figure 4-4). The amount of power output from the test cell increased by about 50%, and was still increasing slightly after 6 days of testing. Because the power output was still quite low, the test was discontinued.

The set of samples manufactured with SS304 (M14-M15) exhibited more corrosion than all other samples. Although in most cases the amount of corrosion was minimal, damage to the monopolar plates and MEAs caused poor cell performance, and in some cases, failure. The amount of rust was not quantified, since any rust formation was considered to be a byproduct of a poorly produced part. Inspection of sample M14, after in-situ testing, revealed that some Fe_2O_3 (rust) was present on the back surface of the plates. This same orange residue was also observed near the inlet flow hole of the cathode monopolar plate. Further investigation revealed that the rust was coming from the humidification system, which was subsequently replaced with a new one. Since initial cell performance was quite low (low conductivity), testing of M14 was not continued.

Rust was also evident on sample M15 after removal from the test cell. While a larger area of rust was found on the backside of the monopolar plate (touching the current collector), a significant amount of the reddish-brown residue was present on the active area of the plate.

The edges of plate M15a had three areas with a large amount of rust on them. Trimming the edges of the plates, to fit in the fuel cell base, exposed a higher concentration of fibers to the moist conditions of the fuel cell. Ideally, the edges of the plates would not be in contact with water from the fuel cell and gasketing would keep all water internal to the system. However, the compression fit method of securing the monopolar plates in the test fuel cell allowed an interface between the edge of the plate and fuel cell body where water could collect and promote rusting. Evidence of rust formation can be seen on the fuel cell body and current collector in Figure 4-9.

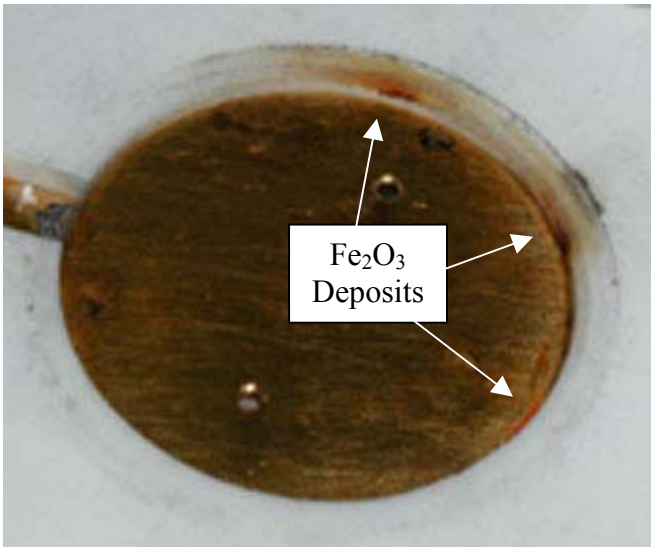

Figure 4-9: Current collector and fuel cell base with Fe_2O_3 deposits from sample M15a.

Rust was also present on the MEA after removal from the test cell (Figure 4-10). Iron oxide is a contaminant of fuel cell membranes, and probably would have caused the membrane to fail.

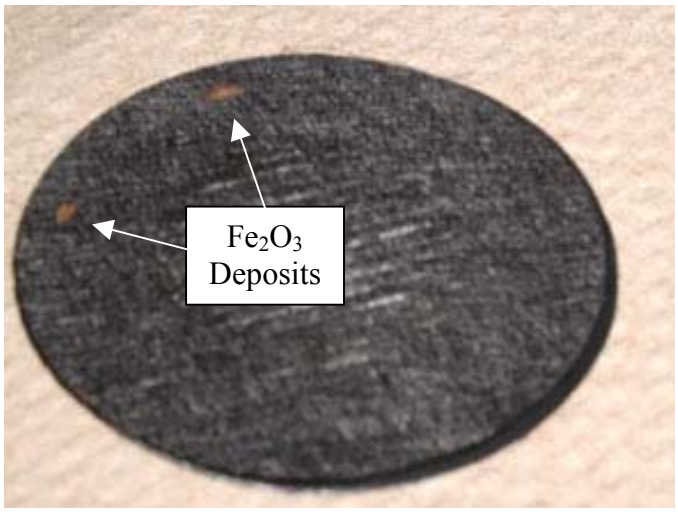

Figure 4-10: MEA with Fe_2O_3 deposits from composite plate M15a.

A scanning electron microscope (SEM) was used to further investigate and confirm the presence of Fe_2O_3 on the monopolar plates. A surface scan is shown in Figure 4-11, which shows the material build-up on the face of the plate at 300x magnification. This layer would certainly increase the resistance in the cell.

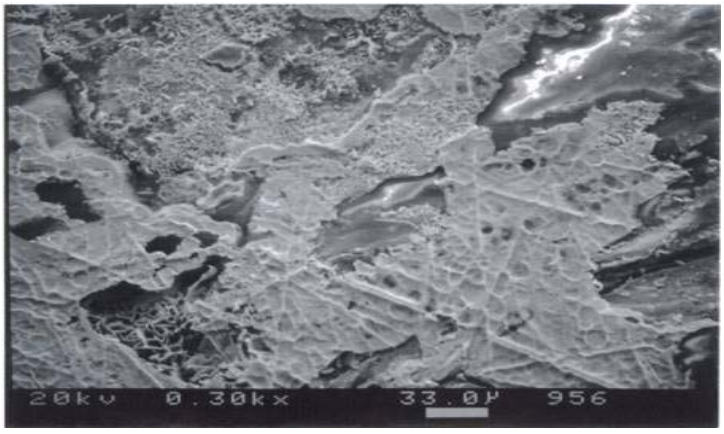

Figure 4-11: SEM of Fe_2O_3 residue on the monopolar plate surface.

After sample M15a had been removed from the test cell, it was sanded down and designated as sample M15a-SM for further testing. This surface modified sample actually rusted less than the unsanded sample M15a. Reasons for this were not clear. However, this sample had the best in-situ performance of any composite materials tested in this research. Surface modification exposed more of the conductive matrix to the monopolar

plate/MEA interface, which lowered resistance in the cell. Sanding smoothed the surface of the plates, which could have allowed a more uniform current density, reducing highly charged areas that may have been more likely to promote oxidation. A more even surface also may have provided better contact in the cell, making it less likely that areas would collect water and promote rust.

Based on conductivity tests, the M15-coin samples should have performed well during in-situ testing, but they did not perform as well as sample M15a. Coining may have actually helped prevent rust from forming on the plates as neither the M15 coin or the M15 coin-SM samples showed much visible rust. Post in-situ analysis (X-ray photoelectron spectroscopy or XPS) of sample M15-coin showed traces of fluorine and an increase of surface bound oxygen. The origin of the fluorine is uncertain (possibly from membrane degradation), but the oxygen could be from a slight oxide layer that was beginning to form on the monopolar plates.

Samples that were not surface modified should have been protected from rust by the thin layer of polymer from the skin core. A problem is that the flow holes in the plates were not integrated into the mold design and therefore had to be drilled by hand. This invasive drilling procedure exposed the metallic matrix directly to the reactant streams. Any possibility of rusting could have been accelerated because of this step in plate processing, although this seems to be contradicted by the fact that the surface modified samples did not exhibit much visible rust.

The final series of plates to be tested, aluminum based M10, M54, and M55, did not experience any significant corrosion, but a passive layer of aluminum oxide was thought to have hurt the performance of these samples. Of all the composite samples tested, the aluminum based had the poorest in-situ fuel cell performance. Sample M10 with Al5056 fibers had an initial power output of just 0.2 Watts, while sample M54 was only able to produce an initial power of 0.13 Watts. The M55 series (M55-coin, and M55-coin/SM) failed to produce any useful power. X-ray photoelectron spectroscopy was used to characterize the surface composition of the M55 samples following in-situ testing. This analysis revealed a difference in oxygen functionality (type of surface bonds) for the in-situ M55 samples when compared to an M55 control sample.[12] This suggests the formation of an in-situ oxide layer. Conductivity was not a good prediction

for in-situ test stand performance. A scatter plot in Figure 4-12 shows the sample conductivity versus average power output from all composite test cells. It is apparent that little if any relationship exists between average power output and initial sample conductivity for this set of samples.

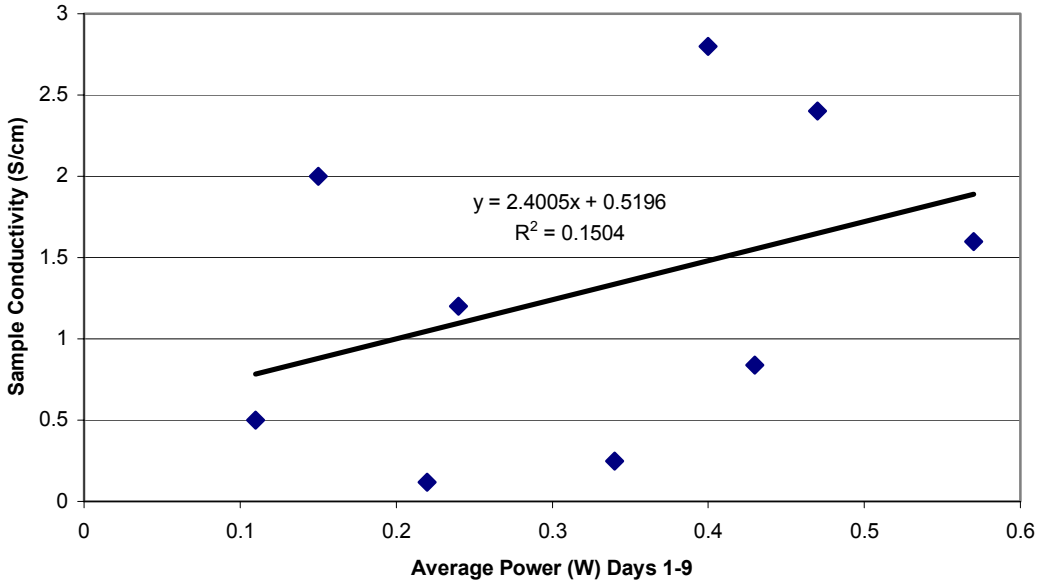

Figure 4-12: Plot of sample conductivity vs. average power output.

In almost all cases, the power output from cells containing composite monopolar plates declined significantly over the duration of the corrosion testing. Scans (XPS) also confirmed the presence of silicone on sample M55 after corrosion testing. Table 4-3 shows the conductivity of the monopolar plates before and after in-situ testing. Conductivity data after corrosion testing further supports the oxide layer theory. After removing the monopolar plate samples, conductivity was tested immediately to insure that measurements reflected conditions upon plate removal. Of the six monopolar plates measured after in-situ testing, plate conductivity dropped an average of 84% from their initial conductivities. Conductivity should relate directly to fuel cell performance, and likely would have shown a good correlation if our testing apparatus had been set up to read in-situ conductivities and interfacial resistances.

Table 4-3: Plate conductivity before and after corrosion testing.

Sample	Composite Materials	Mean Conductivity (S/cm) before testing	Mean Conductivity (S/cm) of anode side after testing (% change)	Mean Conductivity (S/cm) of cathode side after testing (% change)	Hours tested
C10	C/Polymer	1.2	-	-	-
M10	C/Al/Polymer	2.0	-	-	-
M14	C/SS/Polymer	0.12	-	-	-
M15	C/SS/Polymer	0.25	-	-	-
M15a	C/SS/Polymer	0.84	-	-	-
M15a SM	C/SS/Polymer	1.6	0.41 (74.4%)	0.32 (80%)	504
M15 coin	C/SS/Polymer	2.4	0.27 (88.8%)	0.26 (89.2%)	480
M15 coin/SM	C/SS/Polymer	2.8	0.29 (89.6%)	0.40 (85.7%)	360
M54	C/Al/Polymer	0.5	0.08 (84%)	0.12 (76%)	-
M55 coin	C/Al/Polymer	2.6	-	0.34 (86.9%)	-
M55 coin/SM	C/Al/Polymer	3.0	-	0.41 (86.3%)	-

Previous research[11] has established that the operating conditions in PEM fuel cells cause passive layers to form even on corrosion resistant metals such as stainless steel. It seems likely then, that such passive layers could have also increased the resistivity of composite materials tested in this research. Gold-plated aluminum monopolar plates were tested by Hentall et al.[7] Performance close to that of graphite was achieved for a short time. Soon after, the performance decreased and it was later discovered that an area of the gold plating had come loose from a plate. The exposed aluminum had contaminated the membrane. This result indicates that aluminum is likely to not perform well as a bipolar plate material and should be avoided in fuel cell systems where MEA contamination may result.

4.3 Estimation of Monopolar Plate Resistance and Error Analysis

In Figure 4-13 are polarization curves for a Poco graphite cell and a cell containing composite sample M15a-SM. The slope of the trend line for the composite sample is slightly steeper than the trend line for the Poco sample. The equations from the linear region of the polarization data indicate that the composite sample test cell has a higher resistance (0.188 Ω) than the Poco graphite cell (0.179 Ω). Although the slope of

the linear region (governed by ohmic losses) is not noticeably different, the equation suggests that a fuel cell stack containing many composite bipolar plates might in fact have a much higher resistance than a cell containing graphite, and therefore, not be able to produce as much current at a given voltage. The location of the polarization curve, shifted down the vertical axis, also indicates that the composite cell will not be able to match the performance of a cell containing graphite bipolar plates.

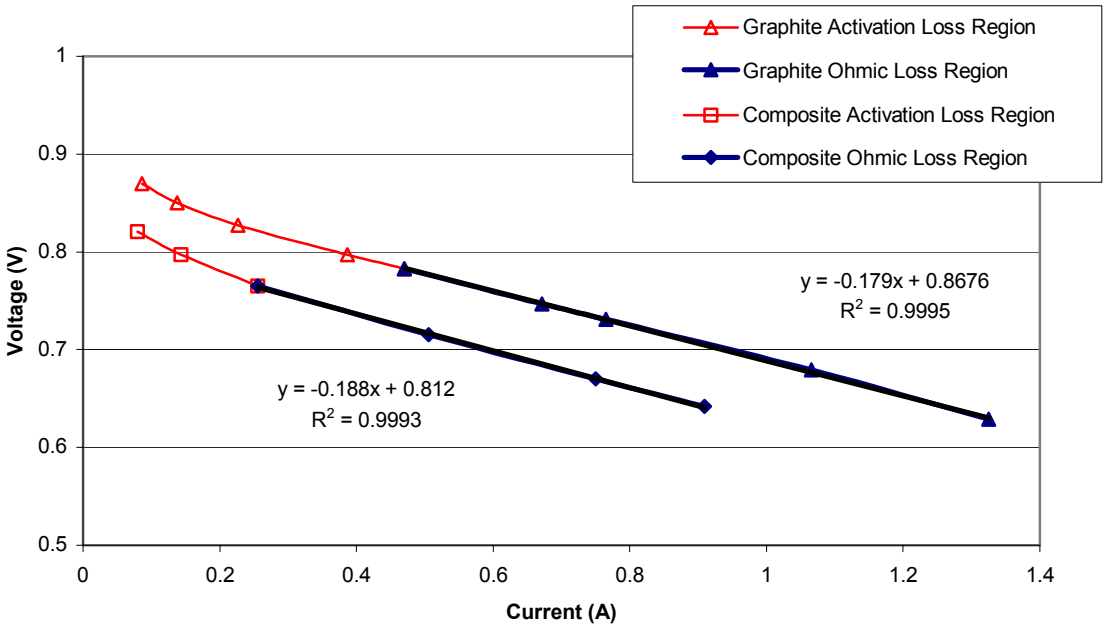

Figure 4-13: Polarization curves comparing a graphite cell to a composite cell. The regions dominated by activation losses are in red (open data points), while the regions dominated by ohmic losses are in blue (closed data points).

Conductivity data was used to calculate actual material resistance for a Poco graphite plate and a composite material plate. Poco plates were machined from 0.064 inch thick graphite and the composite plate was 0.075 inches thick. Based on these values, resistance for the graphite plate and composite plate were calculated as 0.003 Ω and 0.025 Ω, respectively. Since the resolution of the voltage and current meters was only three decimal places, the resistance value for graphite is subjective. However, composite plate resistance represents 26% of the total cell resistance, while the Poco plate accounts for only 3% of the total cell resistance for its respective test cell. Figure 4-14 shows the errors inherent in the voltage and current meter accuracy on a typical polarization curve for composite material plates. Since the error in the voltage

measurements is based only on full scale (of the meter reading), the only change in error occurs in the current measurement. Current readings, for all composite cells, were lower than measurements from the Poco cells, so error bars would be even shorter.

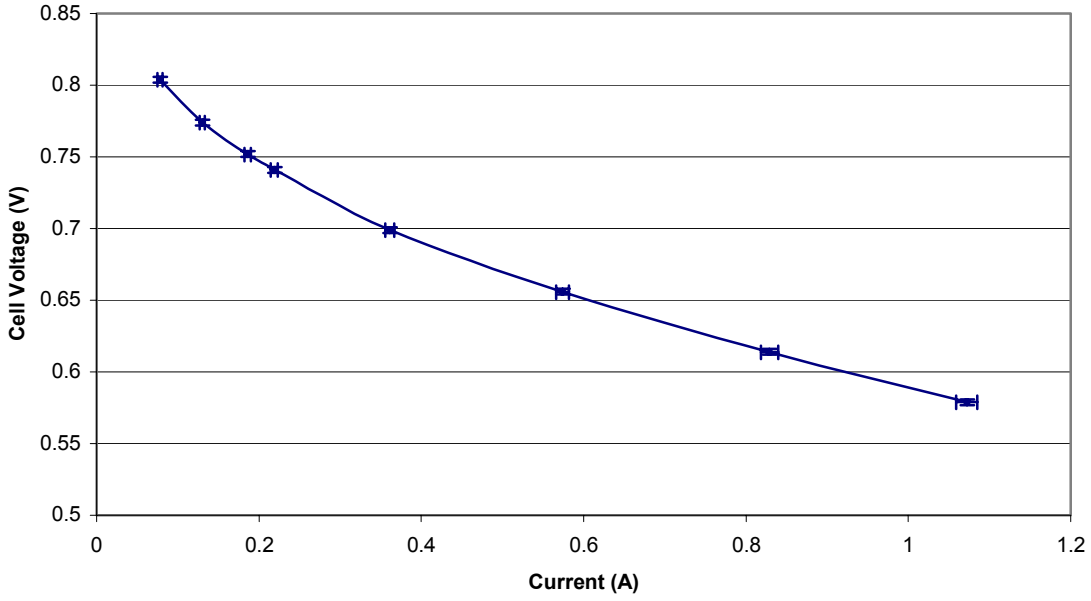

Figure 4-14: Possible error in polarization data from current and voltage meters.

Figure 4-15 depicts a power curve for the average Poco graphite baseline data. Error bars represent the average standard deviation calculated for each of the two baseline cells. Some variability between the readings from both cells caused the standard deviation to be quite large, but in most cases, the values were lower than calculated for the previous baseline data.

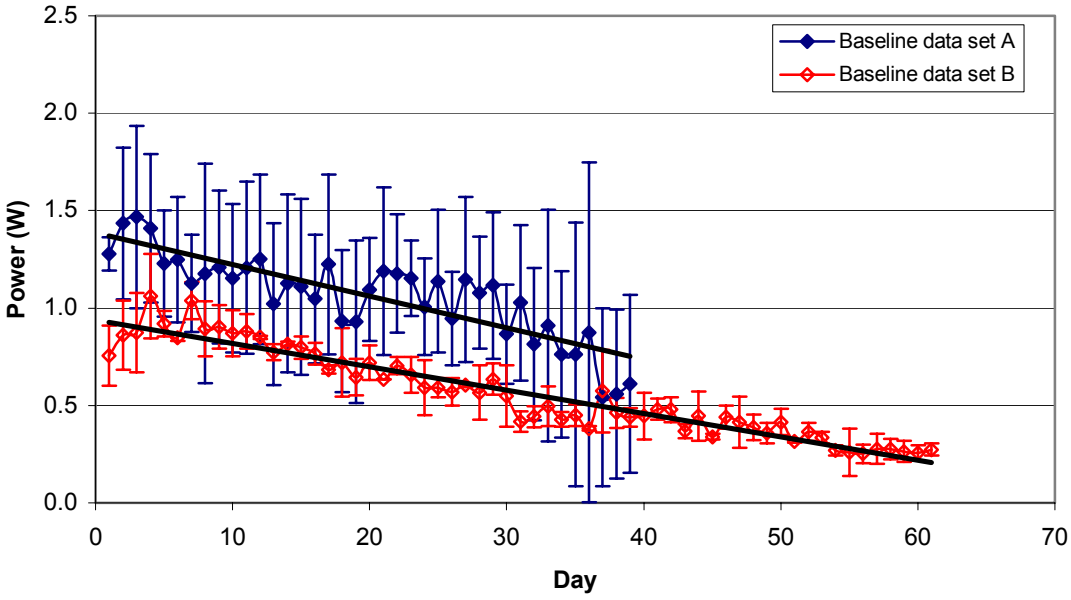

Figure 4-15: Comparison of standard deviation in baseline power data from Poco graphite test cells.

5 Conclusions and Recommendations

This research has shown that the production of injection-coined monopolar plates, for use in PEM fuel cells, is possible at the bench-scale level. A novel process and composite materials were used to successfully manufacture and test monopolar plates for 5cm^2 active area fuel cells.

Conductivity measurements from 137 different composite mixtures were used to screen monopolar plate samples for in-situ endurance testing. Samples were generally not tested unless their conductivities were higher than previous samples. Of the 11 in-situ fuel cell tests, only nine of the cells were able to produce any power using the composite monopolar plates. Samples C10, M10, M14, M15, M15a, M54, M15a-SM, M15-coin, M15-coin/SM were all successfully tested in fuel cells, while samples M55 and M55-coin did not function. Aluminum based composites, M10 and M54, were the lowest performing samples. Test cells containing these samples were able to produce only 10 – 27% of the power that was output by cells containing Poco graphite. The poor performance of all aluminum-based samples, despite high conductivity measurements, indicates this material is not a good candidate for use in PEM fuel cells due to formation of aluminum oxide.

The coined samples in the M15 series had high conductivities relative to the other samples, but power output was less than the cell containing sample M15a-SM. The most promising sample (M15a-SM) was able to produce 50-79% of the power output of a Poco graphite cell. If injection-coining and composite materials dramatically reduce the cost[12] of bipolar plate manufacturing, then generating around 80% of baseline power in cells with composite plates might be acceptable in automotive applications.

5.1 Future Research

Since sample M15a-SM had the best performance on the test stand, future research should look at altering the processing parameters to further improve conductivity. In addition, the feasibility of scale-up to 20-cm^2 active area cells should be explored. If further improvements in conductivity cannot be achieved using current materials, then

alternative polymers might hold promise for future bipolar plate research. Instead of relying on conductive fillers to design the bipolar plates, the use of conductive polymers, such as polysulfones, could improve the plate's electrical characteristics. A new material cost analysis would have to incorporate the probable higher cost of conductive polymers.

Rust occurred on many of the samples that contained stainless steel. Preventing this oxidation should be a major goal of any future research involving this material. Drilling the flow holes into the monopolar plate and cutting the runner from the finished part exposed steel fibers from beneath the protective skin-core of the polymer. A new mold should incorporate the flow holes and possibly have a smaller runner (in relation to the thickness of the plate) to help prevent exposing the metal matrix when readying the part for the fuel cell. Because 304 stainless steel exhibited characteristics of rust in some composite samples, other types of stainless steel alloy fibers (316L, 310, 904L) should be investigated.

5.2 Improvements to the Test Stand

In order to improve the reliability of the fuel cell test stand and improve data collection, some improvements should be made if further testing takes place. The most important improvements would be to the humidification system. It is possible that the high temperatures and the stainless steel tubes used for holding water caused rust to form and contaminated the fuel cell MEAs. Perhaps some sort of ceramic chamber would help eliminate the possibility of rust in the system. A second improvement would be to use a much larger humidification container for holding water. A larger container would prevent large changes in humidity from occurring as in the current configuration, which allows the water level to drop quite significantly between refills. This fluctuation in water level could have helped degrade the MEAs by continually changing the level of membrane hydration. The PID temperature controllers, currently in use on the test stand, should also be upgraded. Failure of the mechanical relays caused the circuit to stay closed, allowing the heaters to run continuously. Temperature controllers with solid-state relays, having a longer mean-time-between-failures, would certainly allow for better data collection.

Longer life would prevent the possibility of having to move a cell to another test station if a controller fails in the middle of a test.

Fuel cell construction and assembly is also an area where improvements will help to yield more steady operation. The tube running from the top of the humidifier to the cell causes the air to cool and water to condense in the tube. These small droplets usually ran back into the humidifier, but occasionally blow into the fuel cell. A momentary drop in current followed this sudden water intake. Figure 5-1 shows a 400 second time history of a Poco graphite test cell. A periodic fluctuation in cell voltage can clearly be seen.

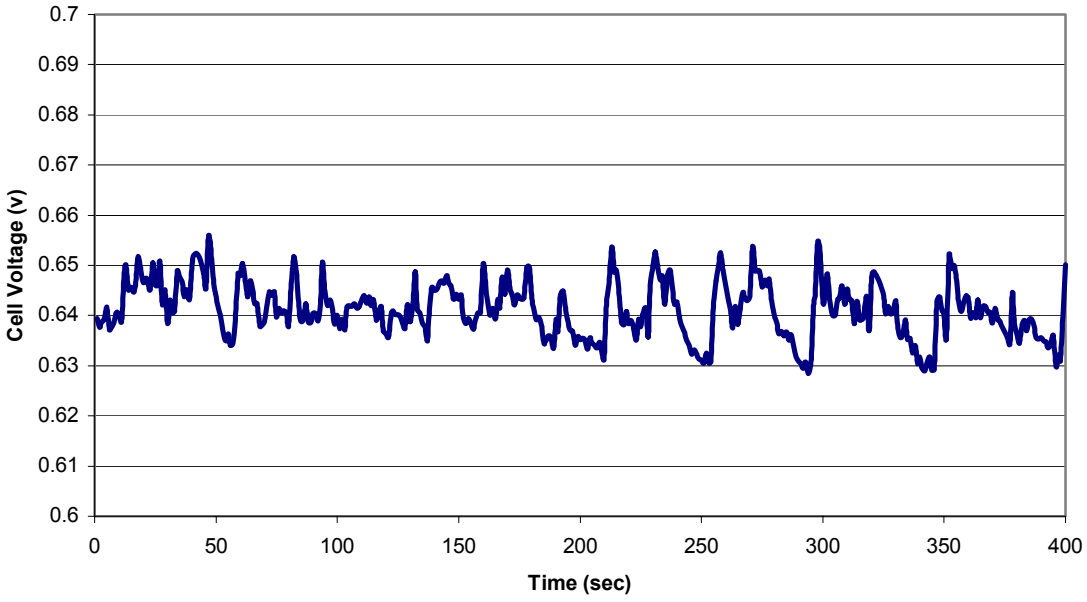

Figure 5-1: Time history of a Poco graphite test cell showing voltage fluctuations.

Repeated exposure to water droplets could have degraded the MEA and contributed to the decrease in power output. A shorter, insulated (or heat traced) tube would eliminate most of the large drops from forming on the way to the fuel cell. Some sort of water trap could also be added to the line between the fuel cell and humidification chamber, but additional heat loss would come from the increase in surface area.

6 References

1. Kruszewski, Eric, "Investigation of Graphite Bipolar Plates for PEM Fuel Cell Performance," master's thesis, (Blacksburg, VA: Virginia Tech, 7 September 2000).

2. Besmann, T. M., Klett, J. W., Burchell, T. D., "Carbon Composite for a Fuel Cell Bipolar Plate," *Materials Research Society Symposia Proceedings*, 496 (1998): 243-248.

3. Scholta, J., Rohland, B., Trapp, V., Focken U., "Investigation on Novel Low-cost Graphite Composite Bipolar Plates," *Journal of Power Sources*, 84 (1999): 231-234.

4. Busick, D., Wilson, M., "Development of Composite Materials for PEFC Bipolar Plates," *Materials Research Society Symposia Proceedings*, 575 (2000): 247-252.

5. Hornung, R., Kappelt, G., "Bipolar Plate Materials Development Using Fe-based Alloys for Solid Polymer Fuel Cells," *Journal of Power Sources*, 72 (1998): 20-21.

6. Davies, D. P., Adcock, P. L., Turpin, M., Rowen, S. J., "Bipolar Plate Materials for Solid Polymer Fuel Cells," *Journal of Applied Electrochemistry*, 30, Part 1 (1999): 101-105.

7. Hentall, Philip L., Lakeman, J. Barry, Mepsted, Gary O., Adcock, Paul L., Moore, Jon M., "New Materials for Polymer Electrolyte Membrane Fuel Cell Current Collectors," *Journal of Power Sources*, 80 (1999): 235-241.

8. Makkus, Robert C., Janssen, Arno H. H., de Bruijn, Frank A., Mallant, Ronald K. A. M., "Use of Stainless Steel for Cost Competitive Bipolar Plates in the SPFC," *Journal of Power Sources*, 86 (2000): 274-282.

9. Davies, D. P., Adcock, P. L., Turpin, M., Rowen, S. J., "Stainless Steel as a Bipolar Plate Material for Solid Polymer Fuel Cells," *Journal of Power Sources*, 86 (2000): 237-242.

10. Hodgson, D.R., May, B., Adcock, P.L., Davies, D. P., "New Lightweight Bipolar Plate System for Polymer Electrolyte Membrane Fuel Cells," The 22nd International Power Sources Symposium, Manchester, United Kingdom, 04/09-11/01. *Journal of Power Sources*, 96, no. 1 (2001): 233-235.

11. Wind, J., Späh, R., Kaiser, W., Böhm, G., "Metallic bipolar plates for PEM fuel cells," *Journal of Power Sources*, 105 (2002): 256-260.

12. "Investigation of Novel, Low Cost Materials and Manufacturing Methods for PEM Fuel Cell Bipolar Plates," SBIR Phase II Final Report: Technical and Commercialization Reports, (Arlington, Virginia: Directed Technologies, Inc., 30 July 2002).

Appendix A – Poco Graphite Data and Figures

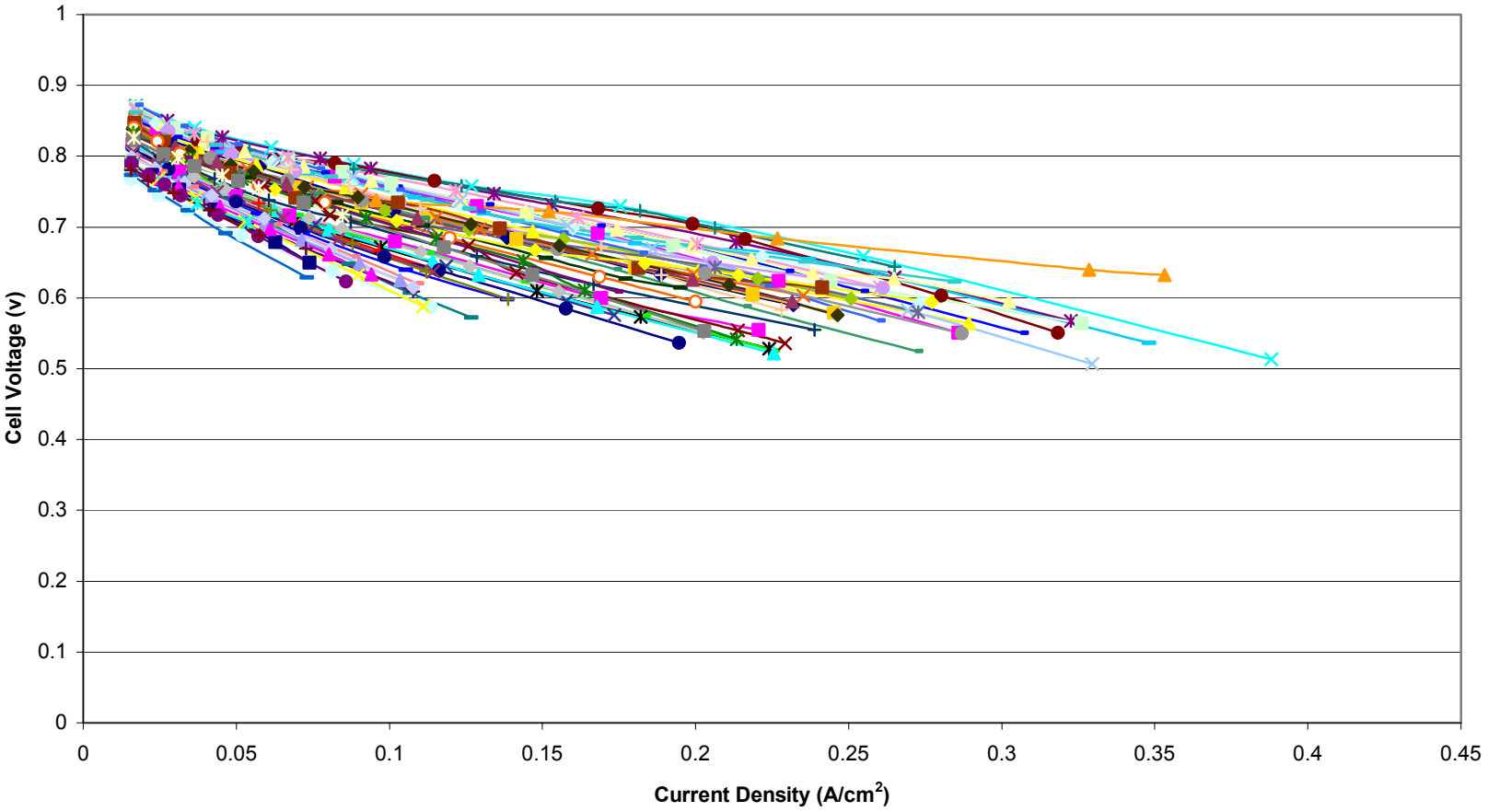

Figure A.1: Polarization curves for Poco graphite baseline cell 1 (Days 1-61).

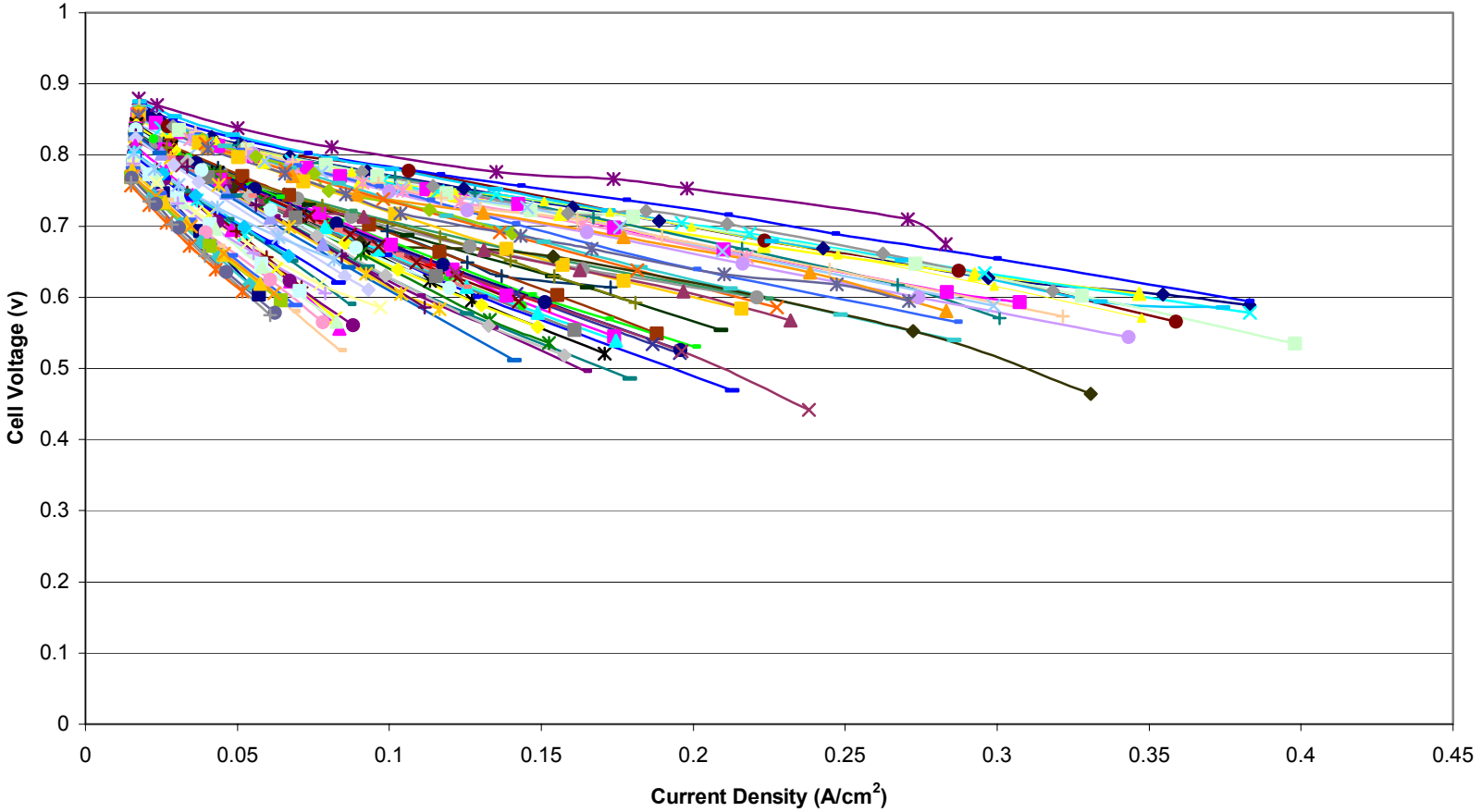

Figure A.2: Polarization curves for Poco graphite baseline cell 2 (Days 1-79).

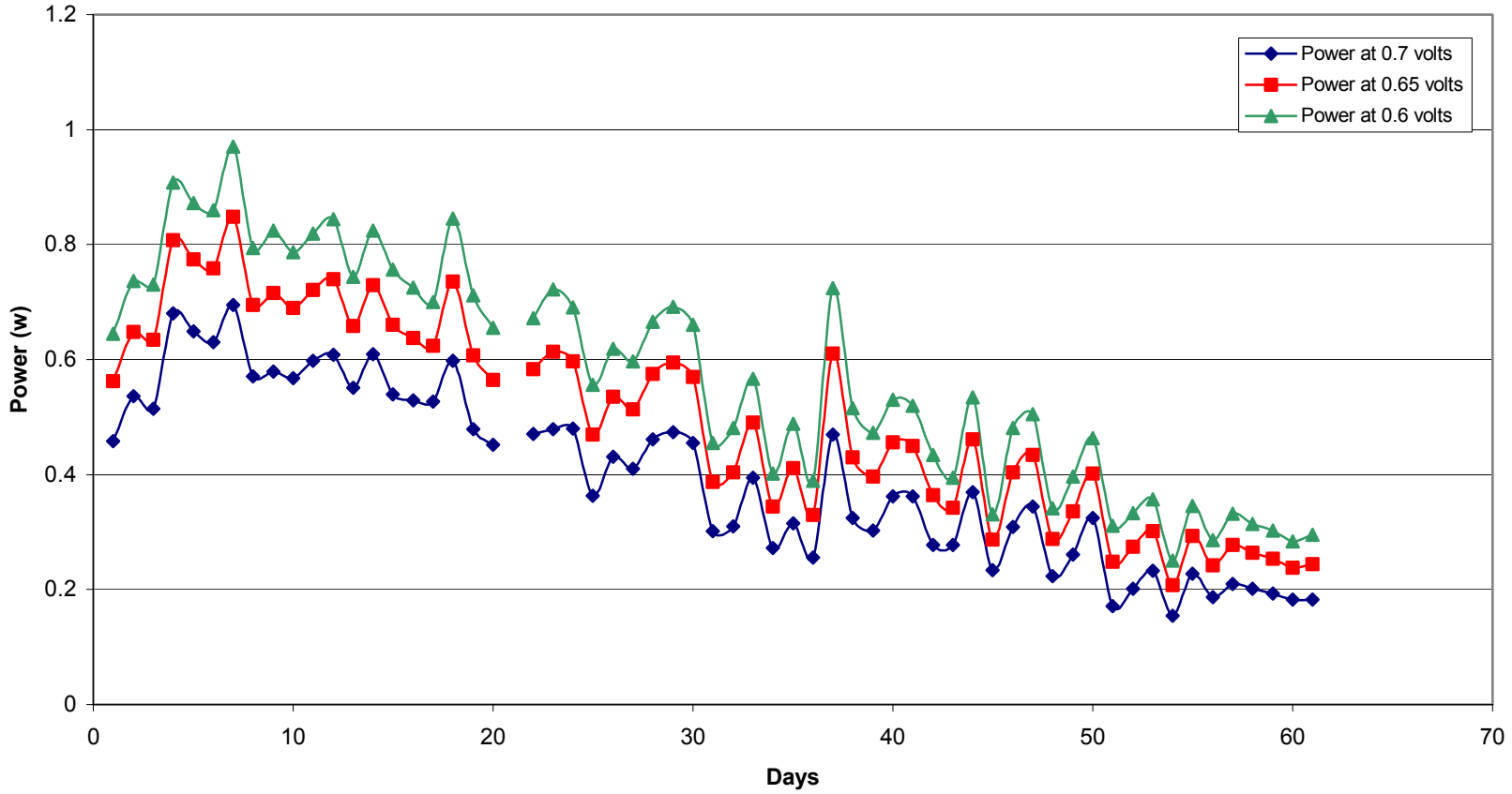

Figure A.3: Power curve for Poco graphite cell 1.

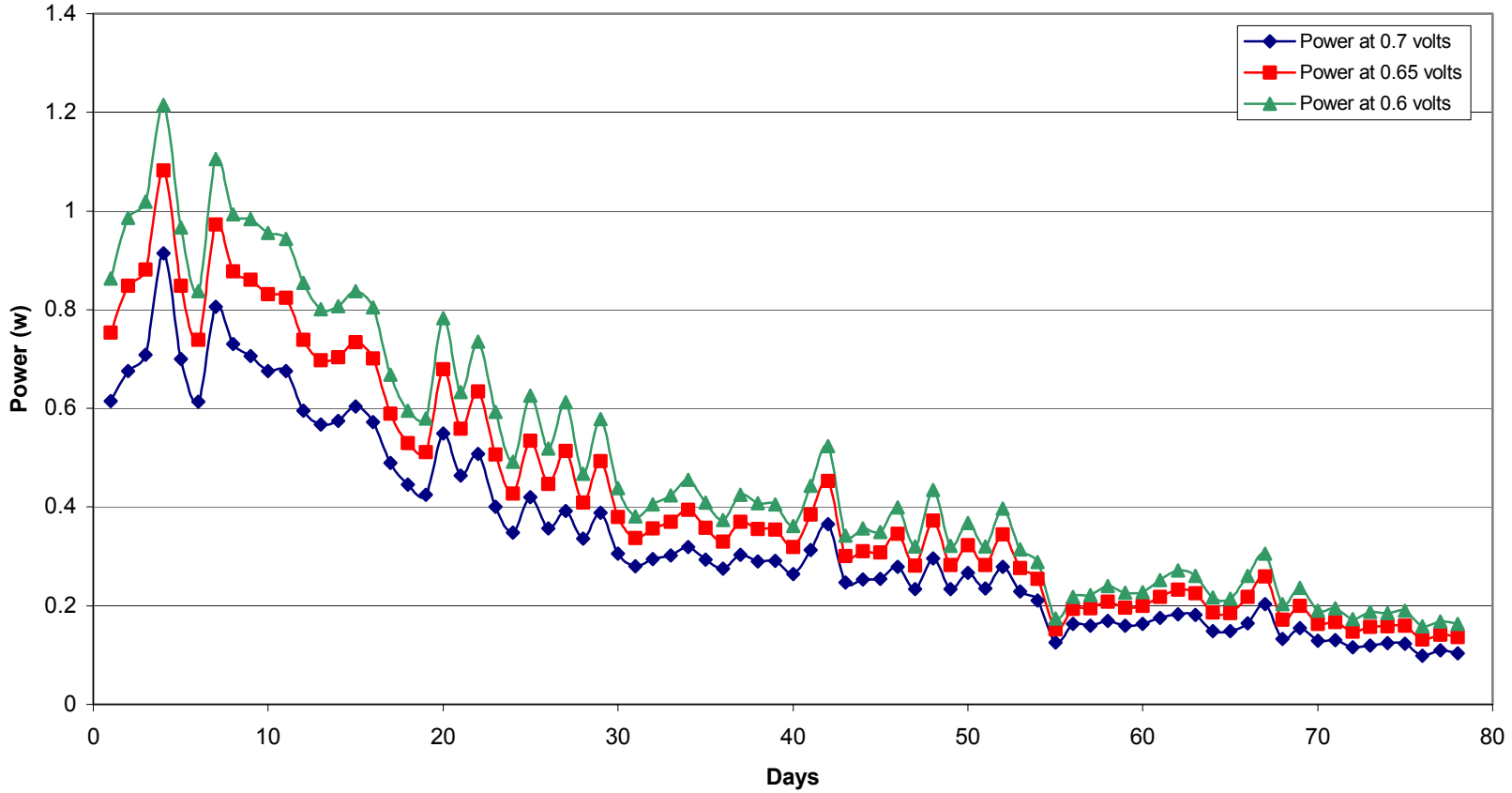

Figure A.4: Power curve for Poco graphite cell 2

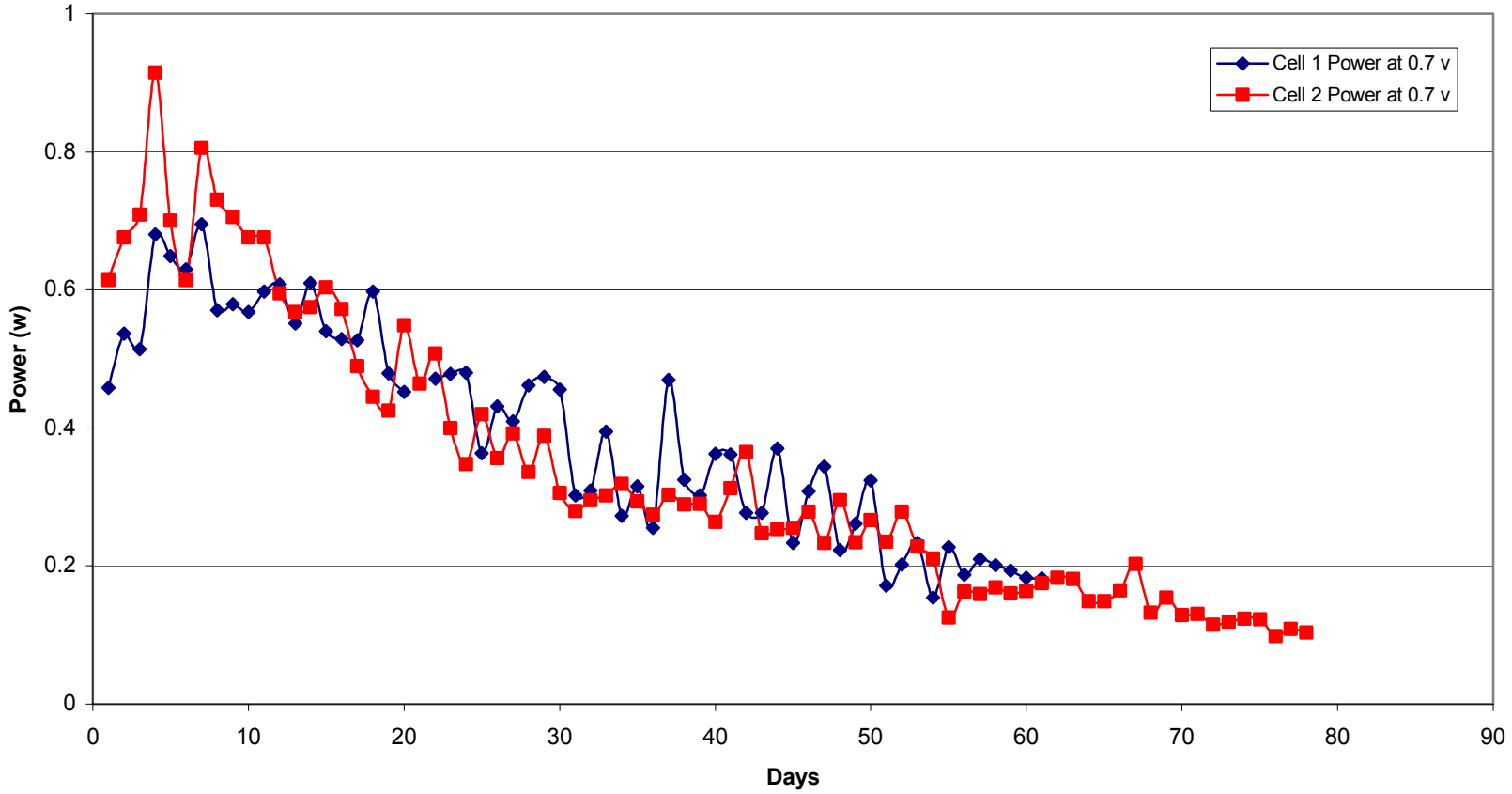

Figure A.5: Power curve comparison for Poco graphite cells 1 and 2 at 0.7 volts.

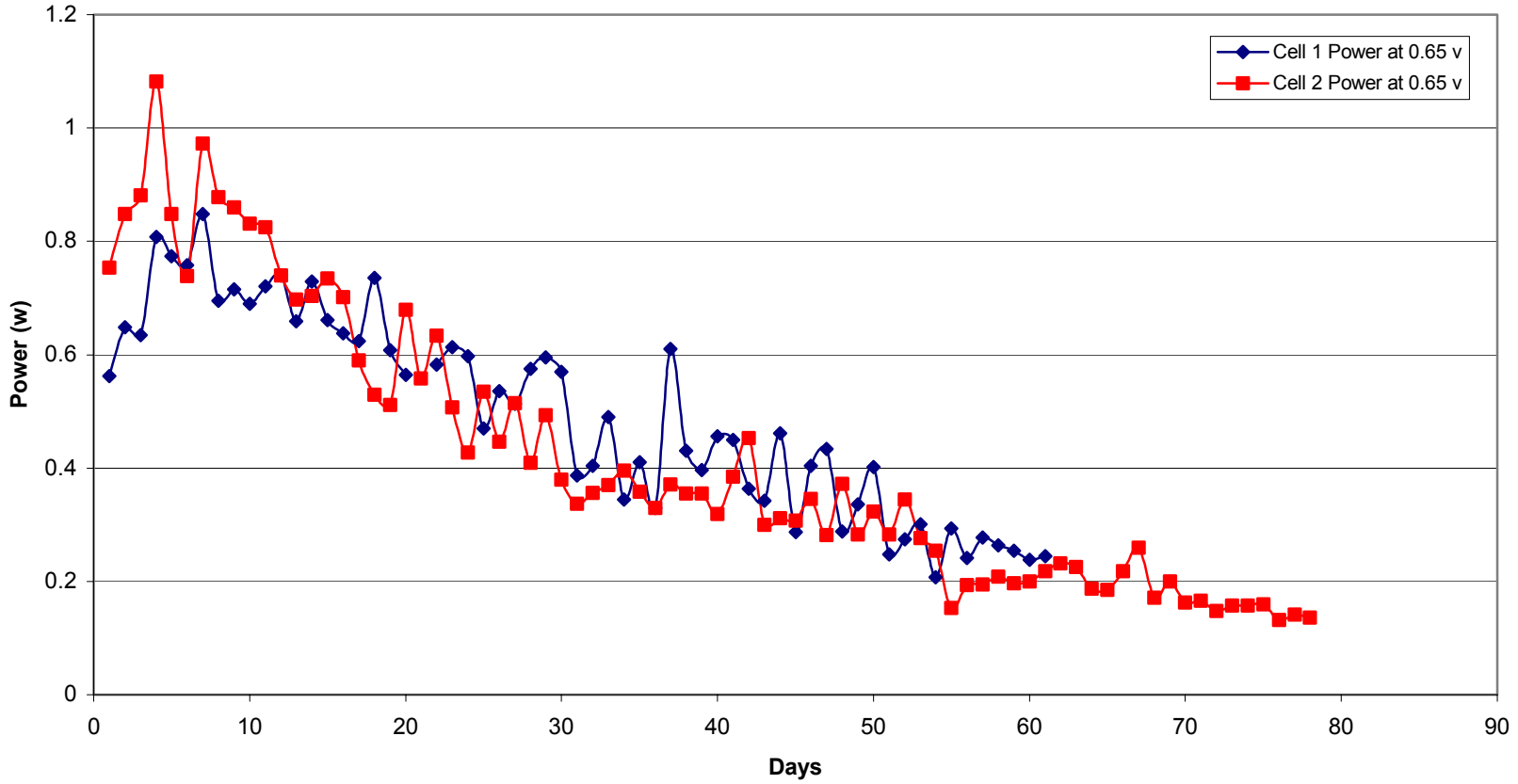

Figure A.6: Power curve comparison for Poco graphite cells 1 and 2 at 0.65 volts.

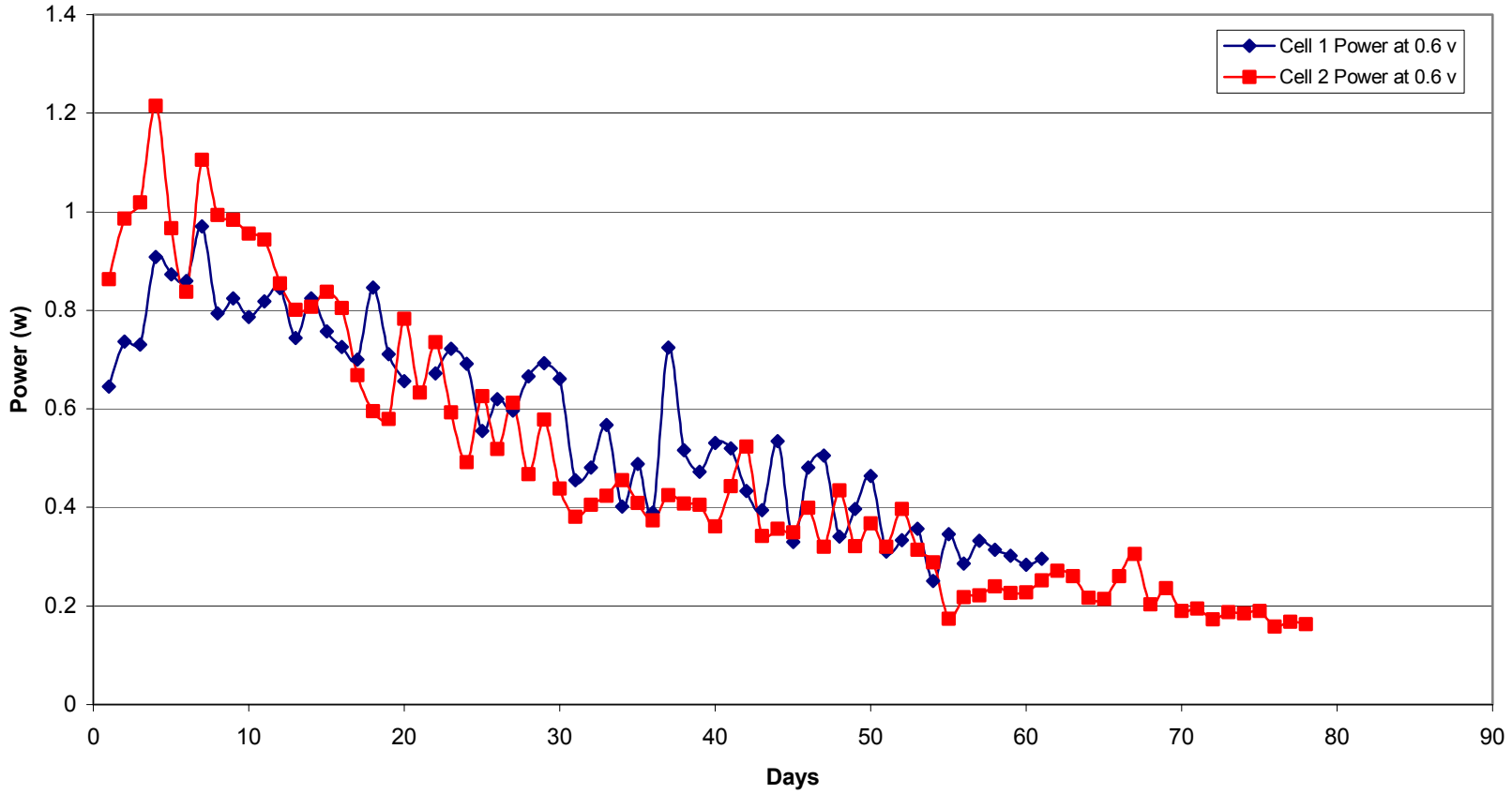

Figure A.7: Power curve comparison for Poco graphite cells 1 and 2 at 0.6 volts.

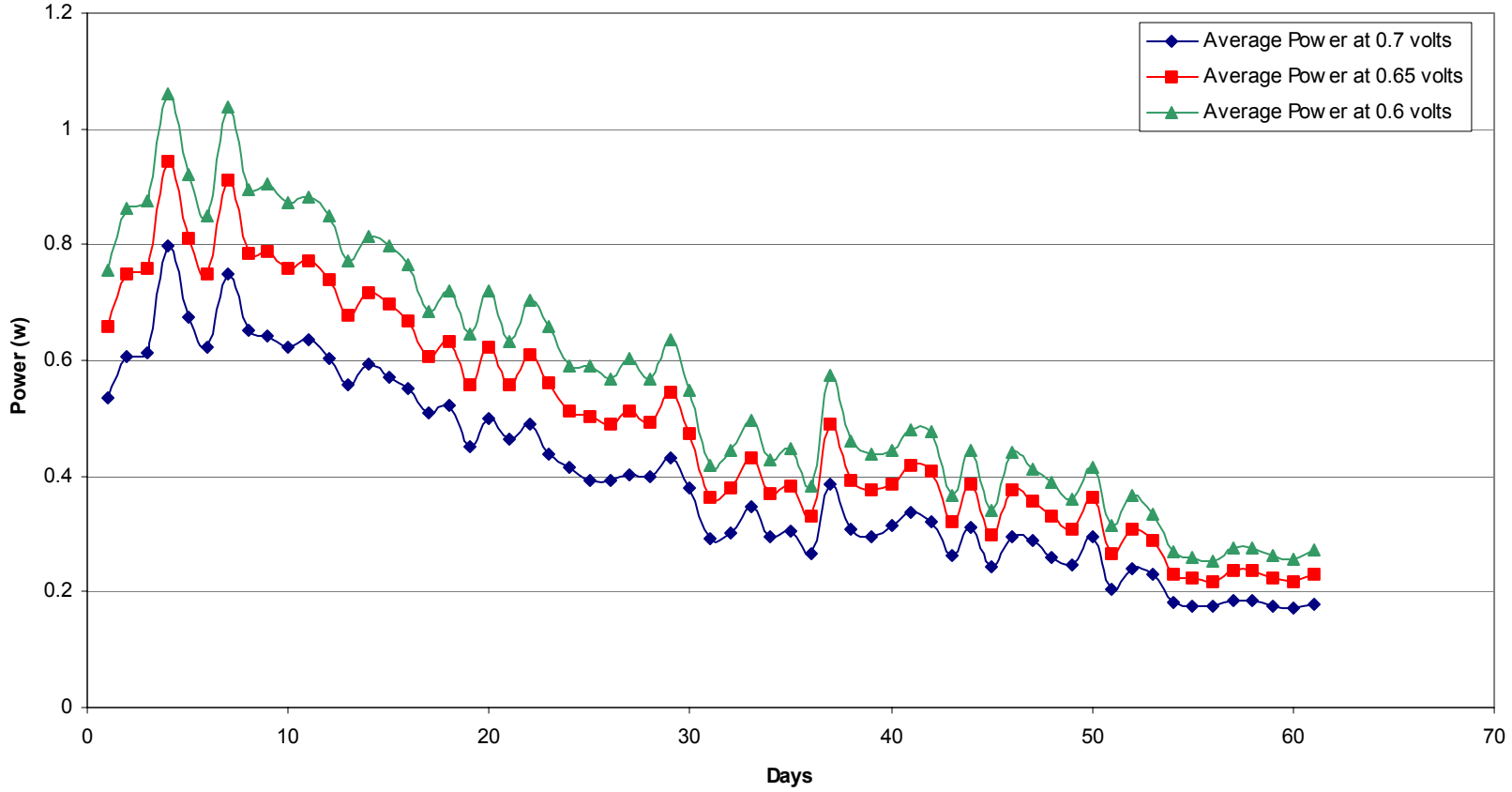

Figure A.8: Average power output from Poco graphite cells at 0.7, 0.65, and 0.6 volts.

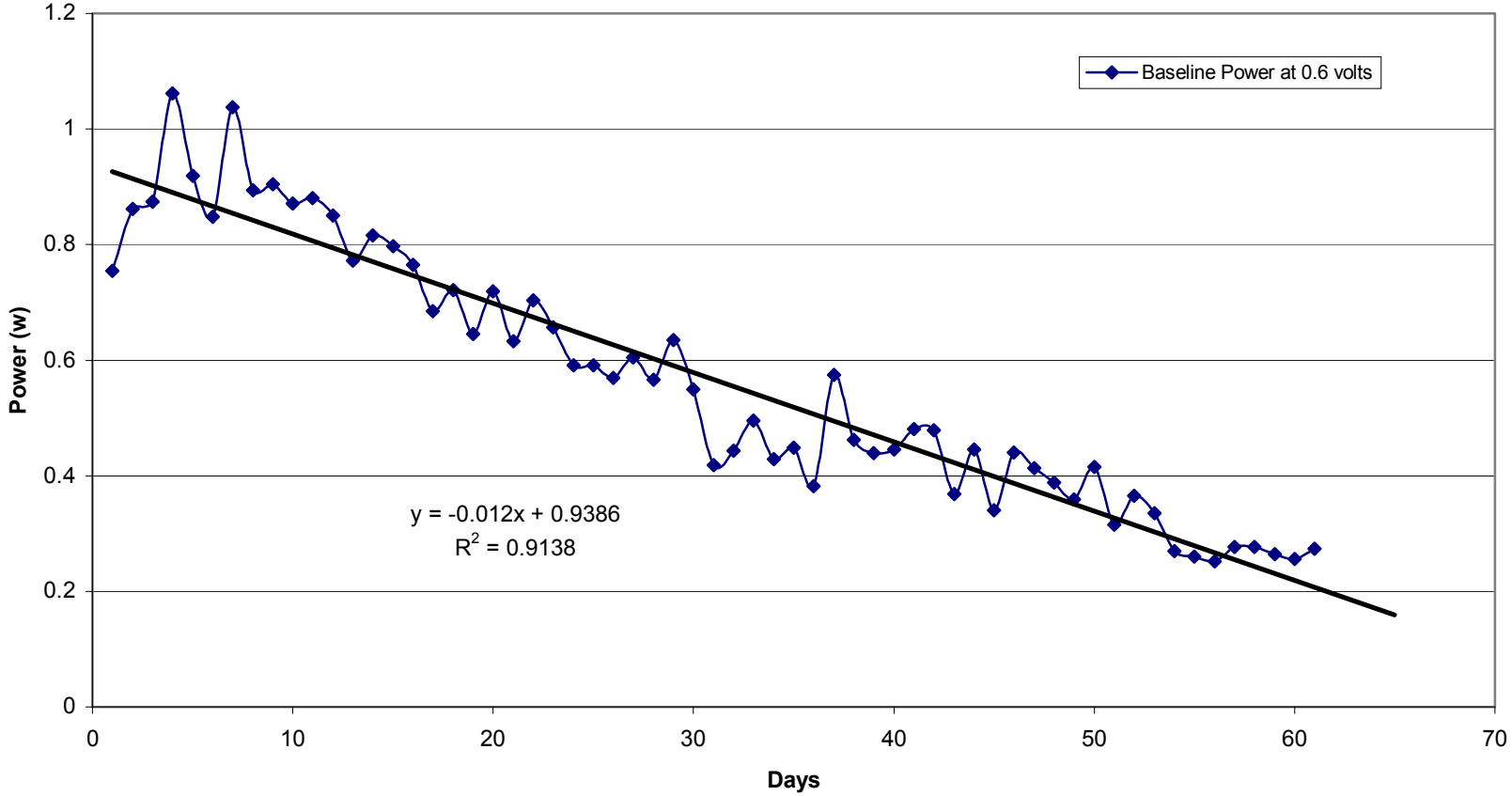

Figure A.9: Baseline data from Poco graphite cells 1 and 2, at 0.6 volts.

Appendix B – Composite Material Data and Figures

Table B.1: Complete composite material monopolar plate data.

Sample	Materials (% volume)				Mean Power Output (W) at 0.6 volts (days 1-9)	Mean Conductivity (S/cm) before testing	Mean Conductivity (S/cm) of anode side after testing (% change)	Mean Conductivity (S/cm) of cathode side after testing (% change)	Hours of testing
	C	SS	Al	PP7200					
C10	50	-	-	50	0.24	1.2	-	-	864
M10	5	-	23[a]	72	0.15	2.0	-	-	168
M14	20	13	-	67	0.22	0.12	-	-	624
M15	20	16	-	64	0.34	0.25	-	-	360
M15a	20	16	-	64	0.43	0.84	-	-	216
M15a SM	20	16	-	64	0.57	1.6	0.41 (74.4%)	0.32 (80%)	504
M15-coin	20	16	-	64	0.47	2.4	0.27 (88.8%)	0.26 (89.2%)	480
M15-coin/SM	20	16	-	64	0.40	2.8	0.29 (89.6%)	0.40 (85.7%)	360
M54	28	-	19[b]	53	0.11	0.5	0.08 (84%)	0.12 (76%)	504
M55-coin	30	-	19[b]	51	0	2.6	-	0.34 (86.9%)	-
M55-coin/SM	30	-	19[b]	51	0	3.0	-	0.41 (86.3%)	-
C = Carbon 4424(50%)/4955(50%), SS = Stainless Steel 304 fibers, a = Aluminum 5056 fibers, b = Aluminum K109 flake, PP7200 = polypropylene									

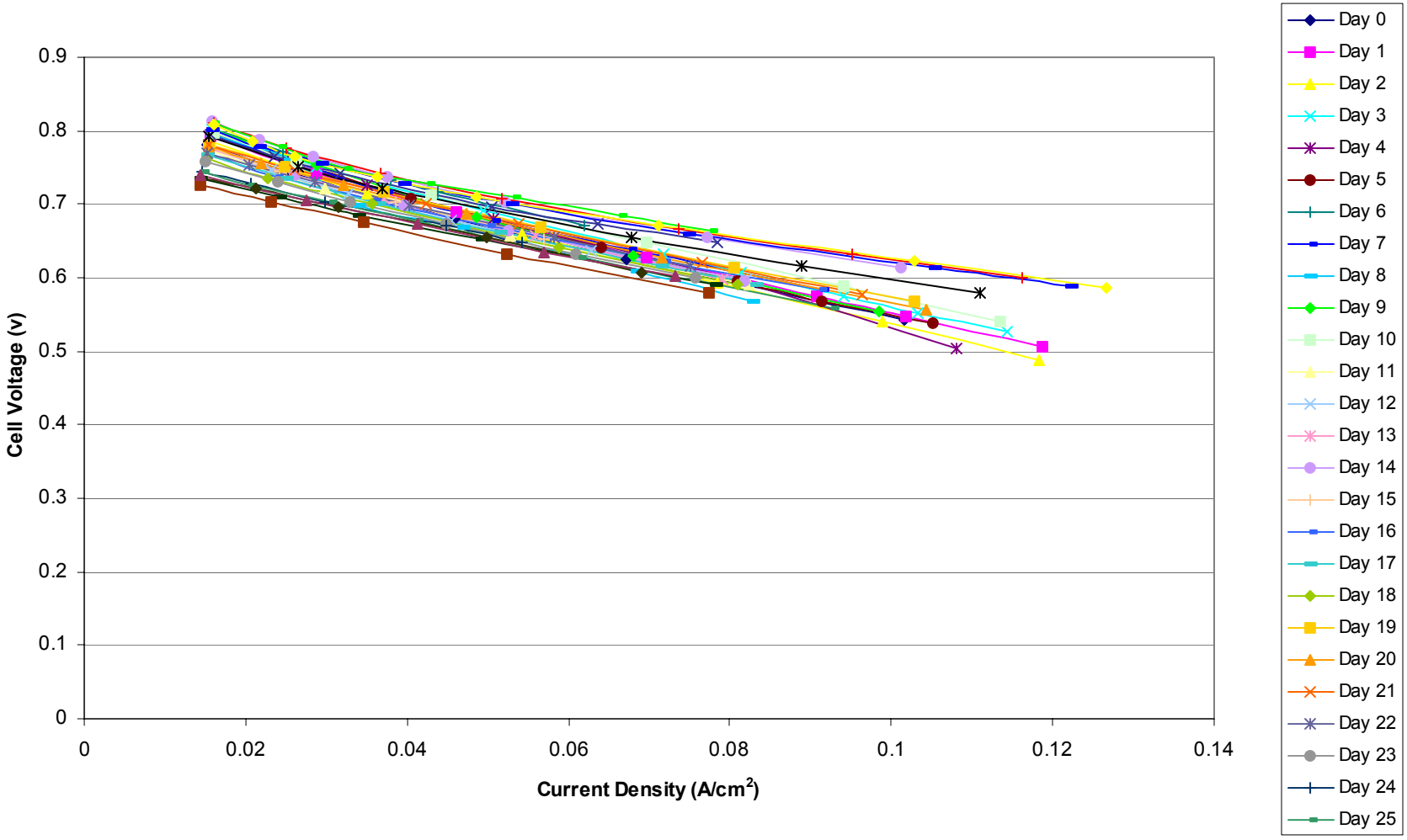

Figure B.1: Polarization curves for sample C10.

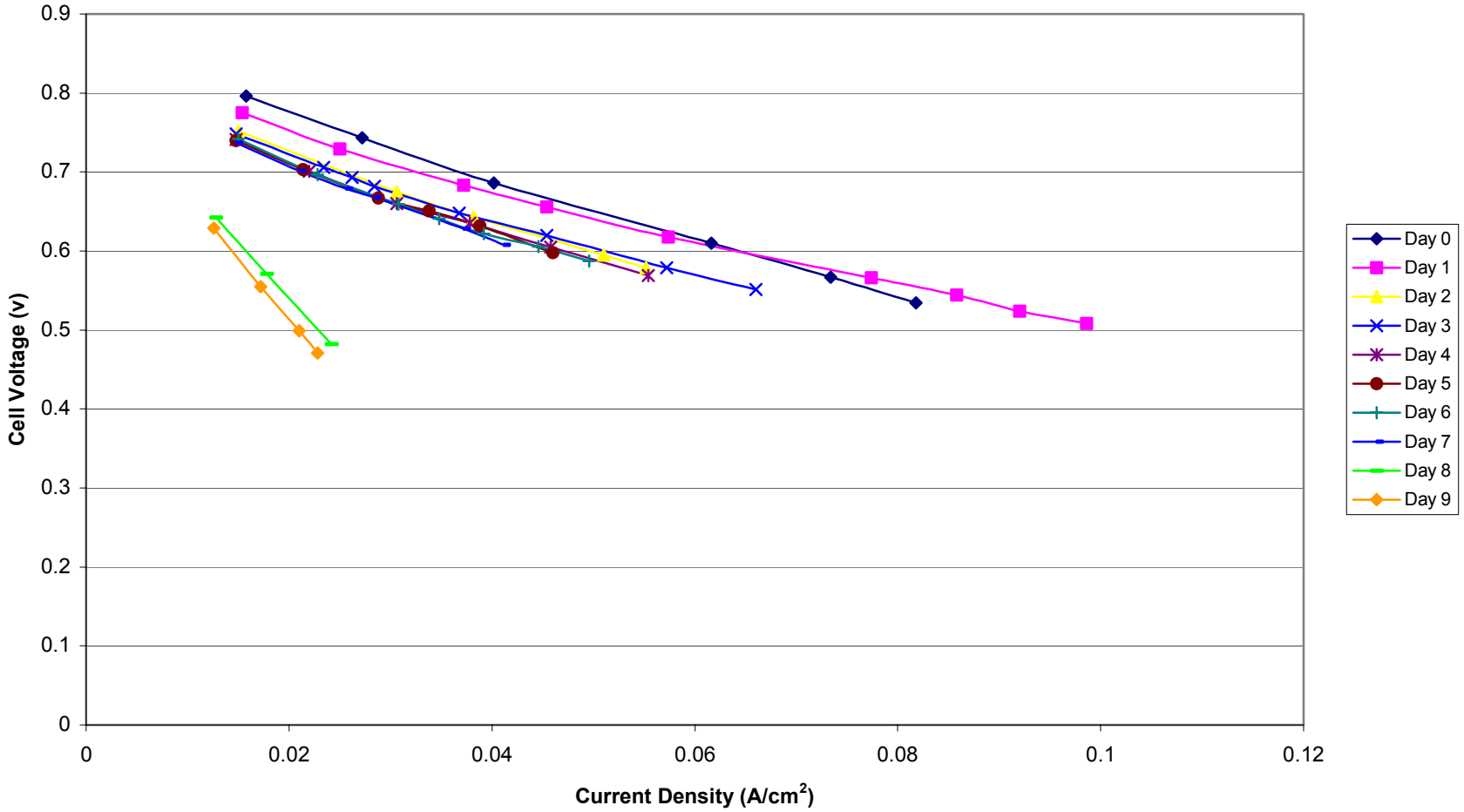

Figure B.2: Polarization curves for sample M10.

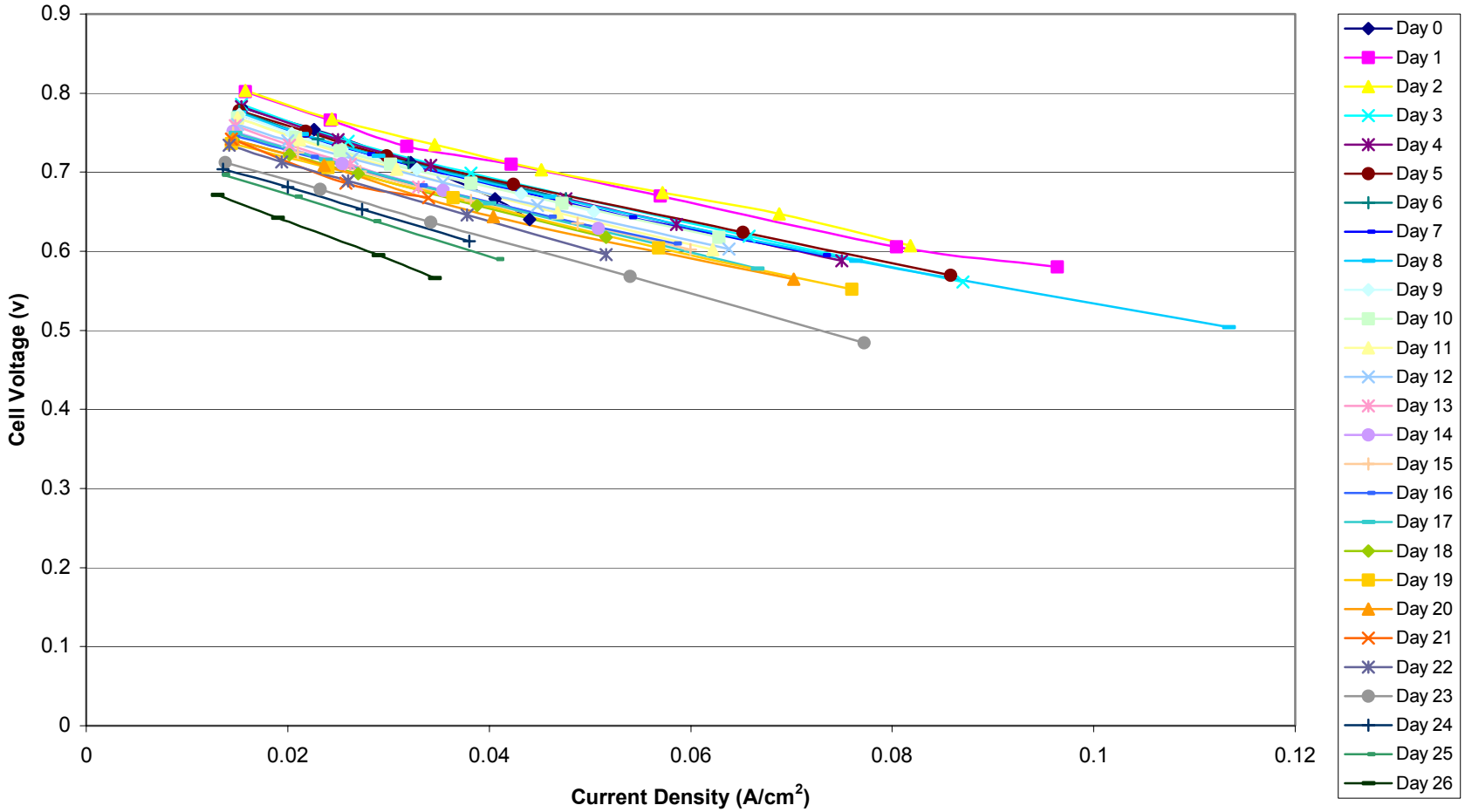

Figure B.3: Polarization curves for sample M14.

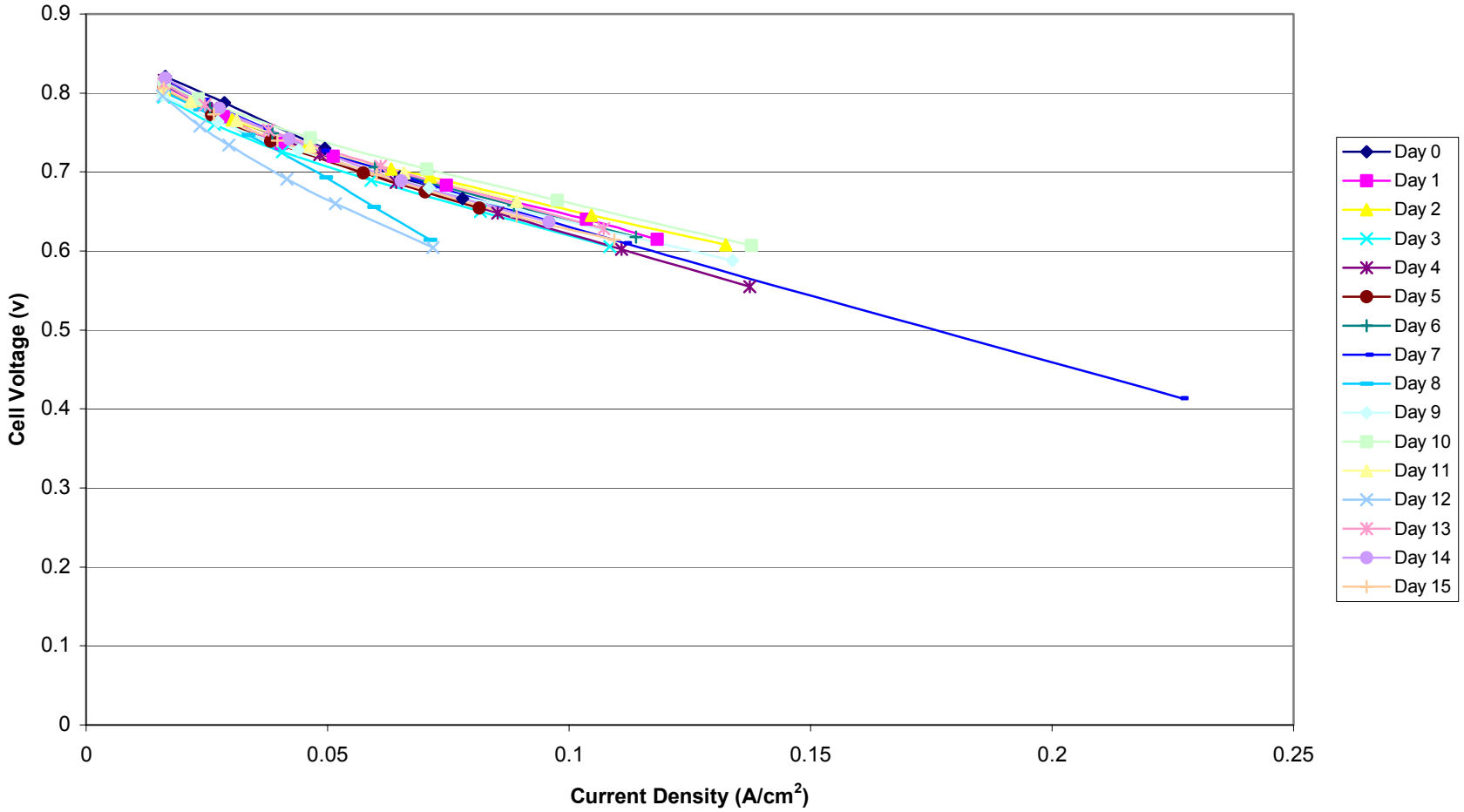

Figure B.4: Polarization curves for sample M15.

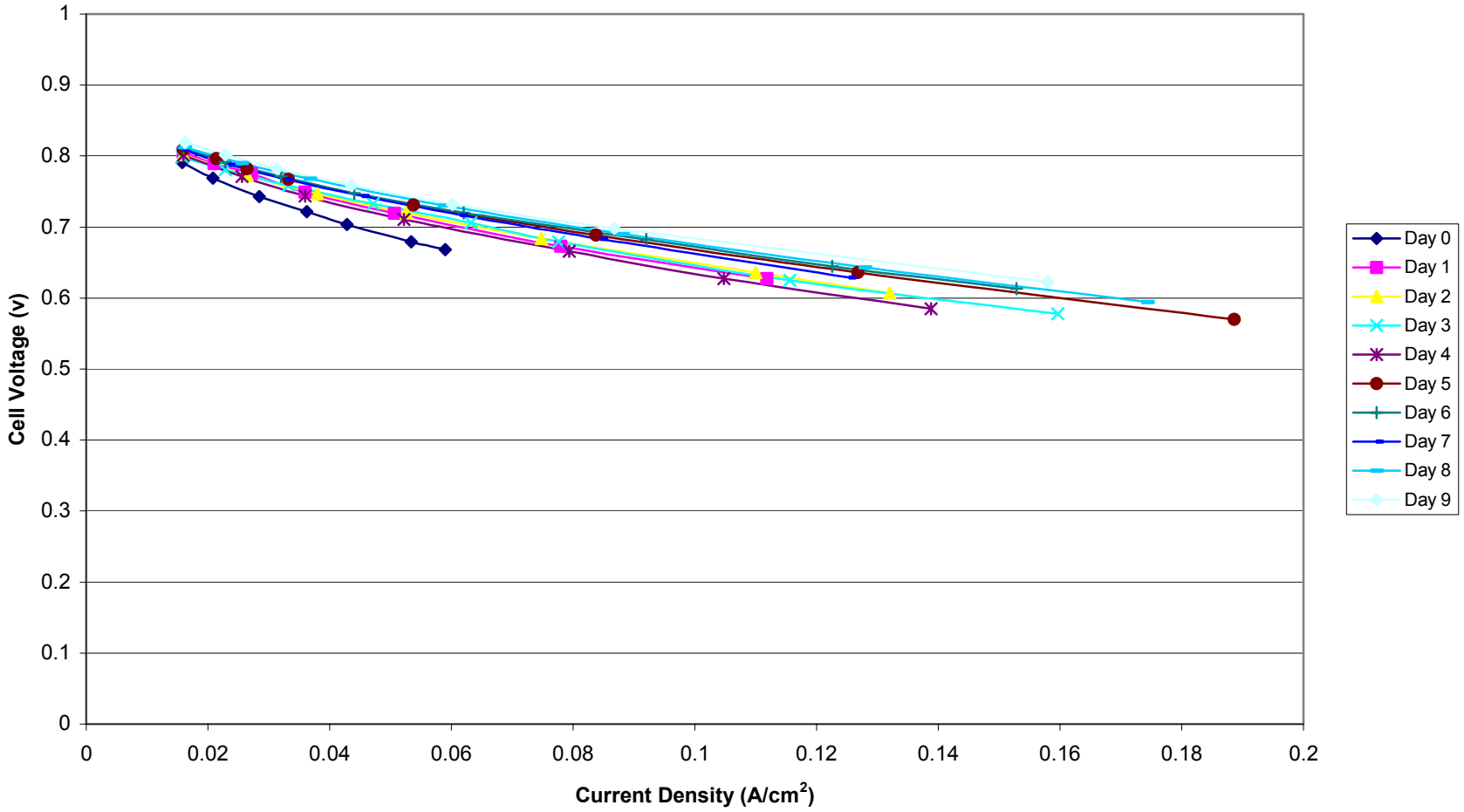

Figure B.5: Polarization curves for sample M15a.

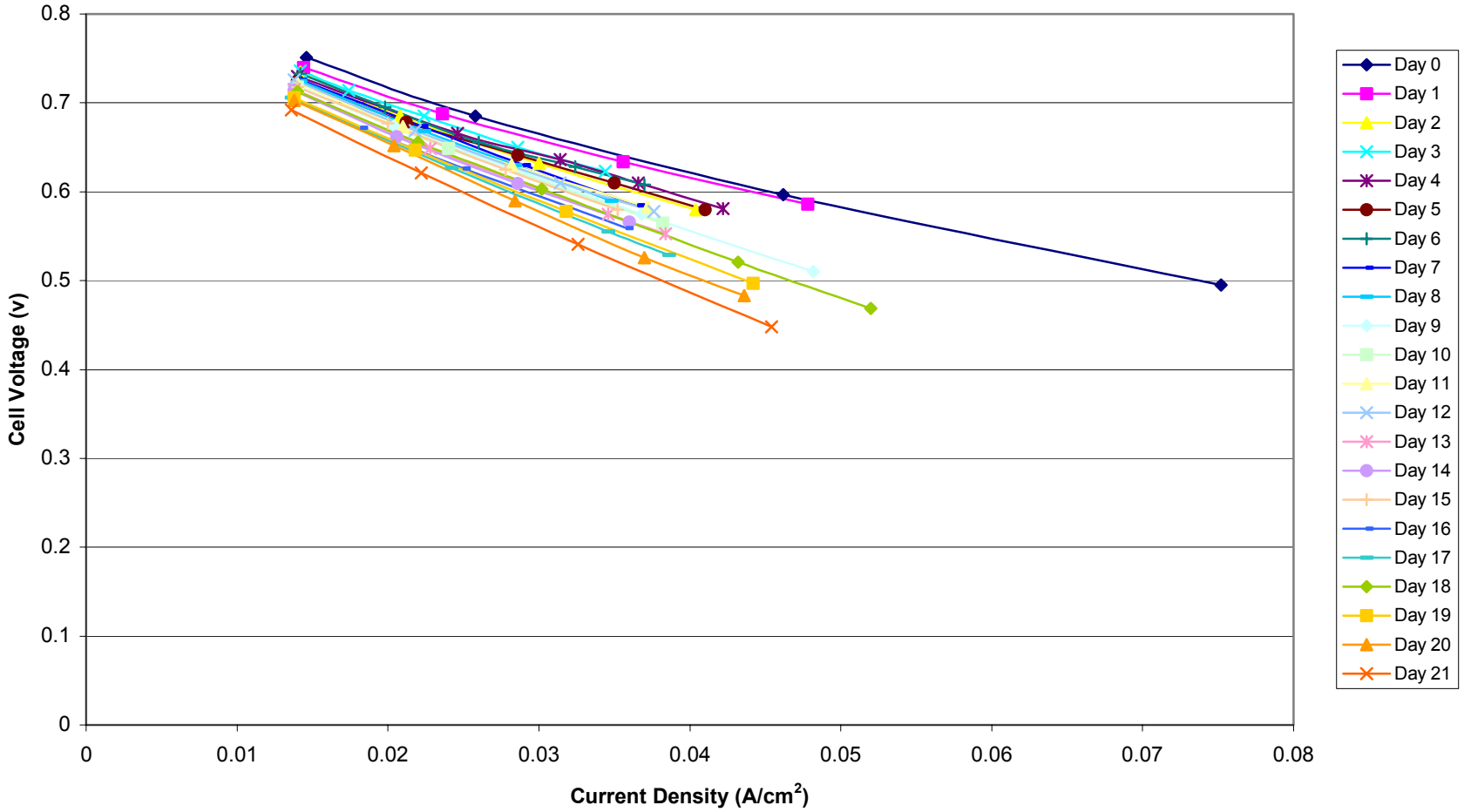

Figure B.6: Polarization curves for sample M54.

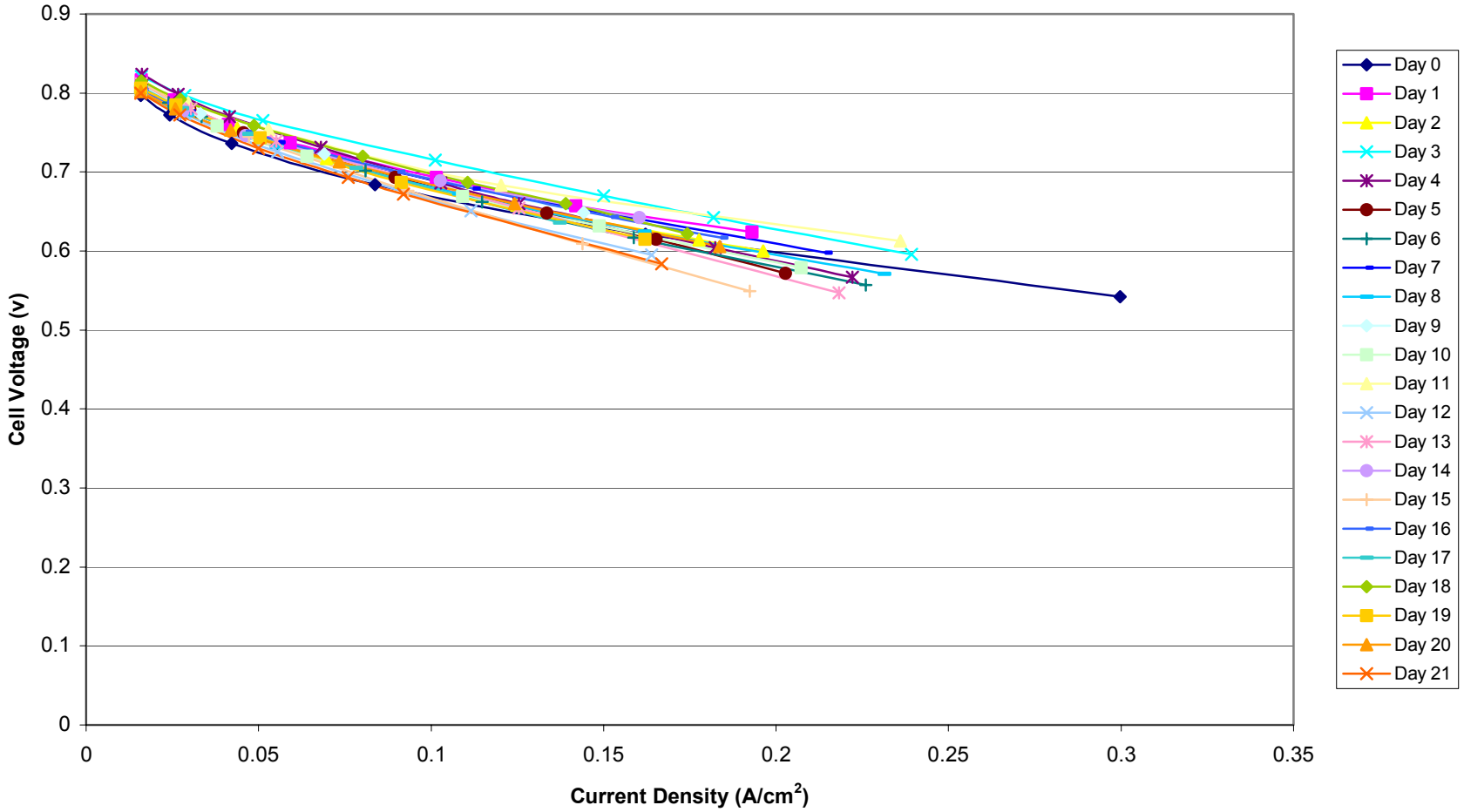

Figure B.7: Polarization curves for sample M15a-SM.

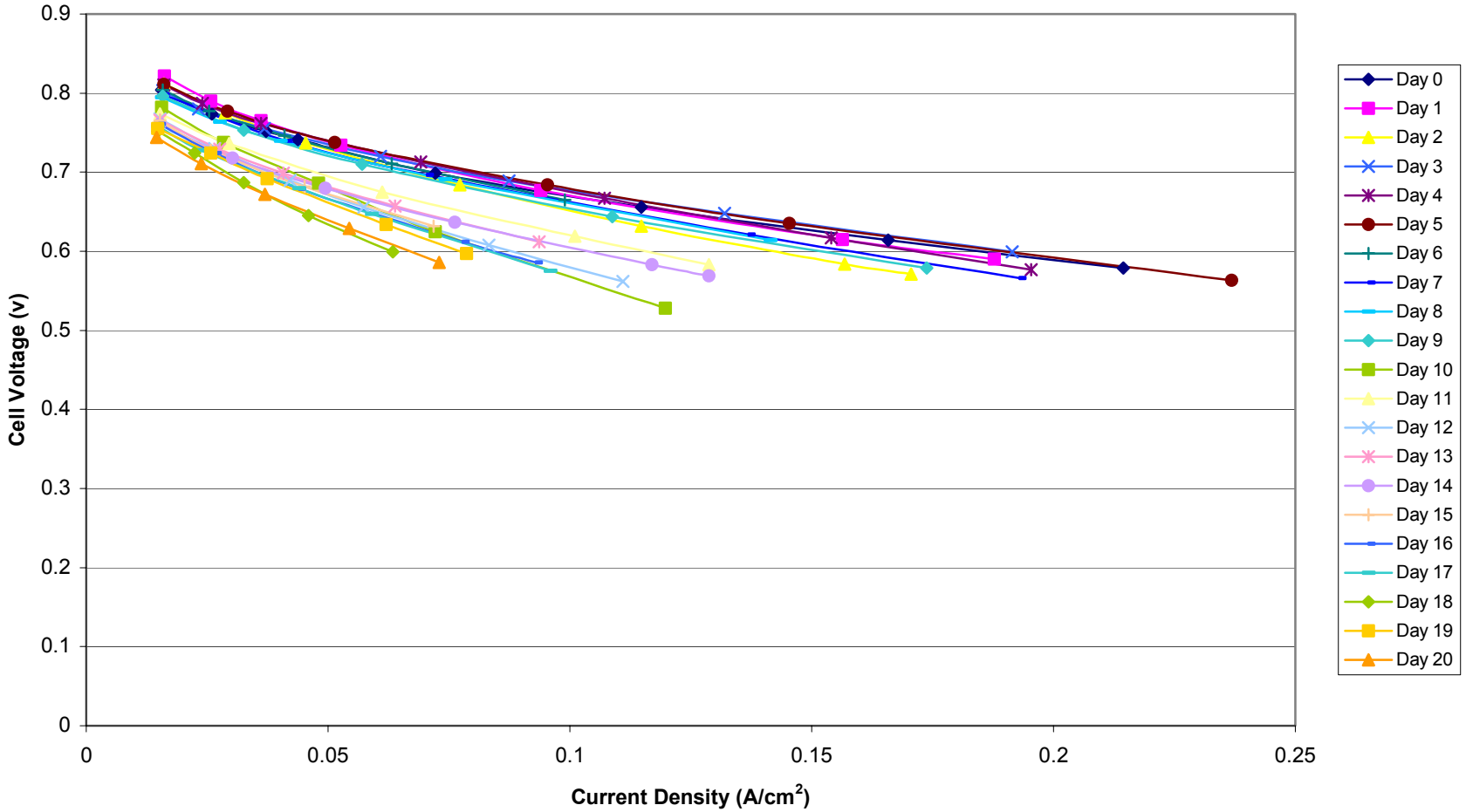

Figure B.8: Polarization curves for sample M15-coin.

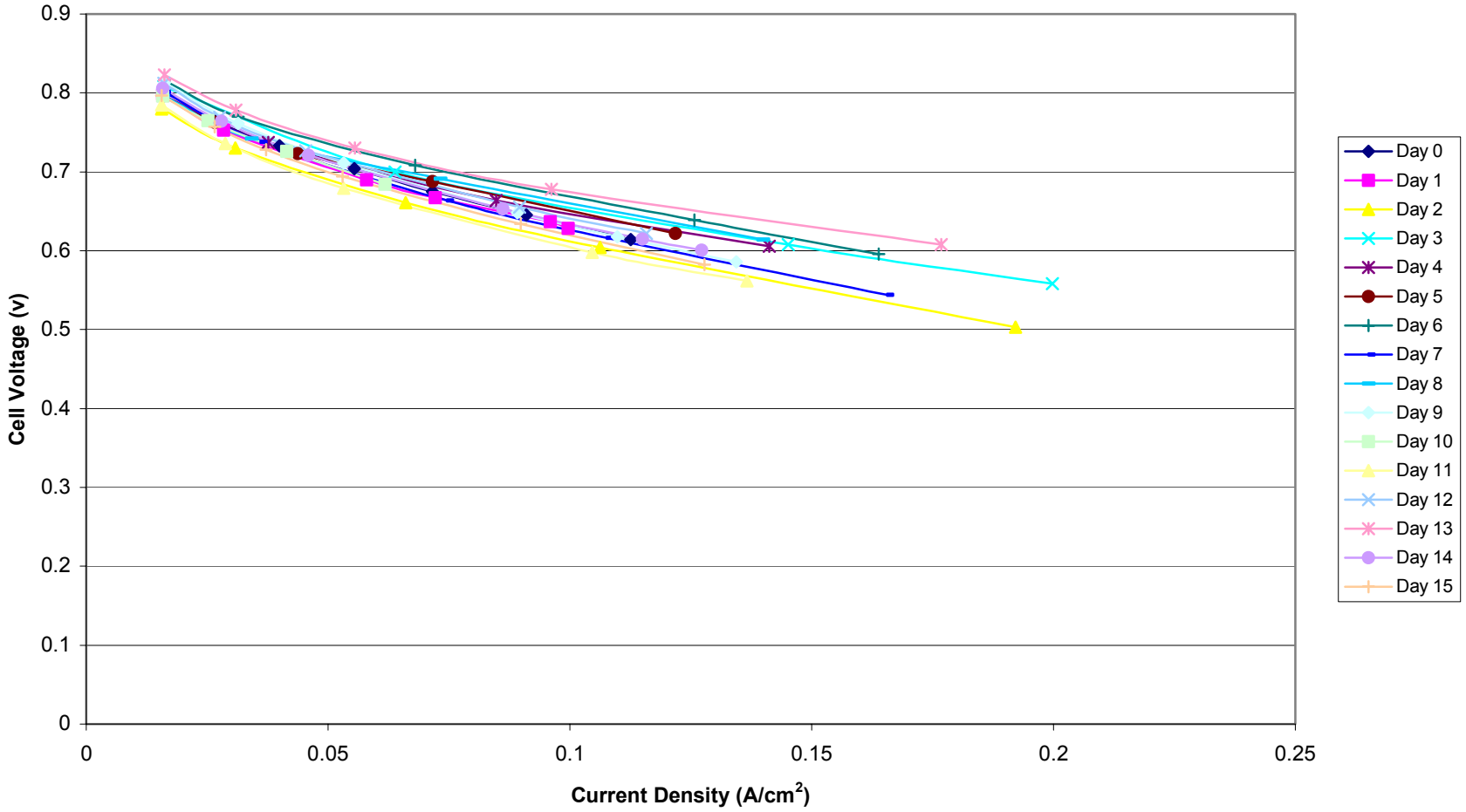

Figure B.9: Polarization curves for sample M15-coin/SM.

Vita

Kevin Campbell Desrosiers

I was born December 2, 1975 in Fresno, California to parents Paul and Barbara Desrosiers. I have one brother, Patrick. After graduating second in my high school class in 1994, I attended California Polytechnic State University, San Luis Obispo (Cal Poly – SLO) and in 1999 earned a Bachelor of Science degree in Environmental Engineering. My senior project dealt with recovering copper ions from semi-conductor process effluent using titanium dioxide photocatalysis. During the spring of 1998, I was selected to attend the first National Science Foundation sponsored Research Experience for Undergraduates (REU) summer program at Clarkson University. There, I helped develop a process for removing arsenic from drinking water sources using membrane filtration technology. An interest in alternative energy eventually led me to Virginia Tech to study fuel cell technology. I joined the Hybrid Electric Vehicle Team and became familiar with fuel cell systems integration, which complimented my research in fuel cell materials.